Efficient Analyses and Models of VLSI and MCM Interconnects *

Andrew B. Kahng and Sudhakar Muddu

UCLA Computer Science Department, Los Angeles, CA 90024-1596
abk@cs.ucla.edu, sudhakar@cs.ucla.edu

Abstract

In performance-driven interconnect design, delay estimators are used to determine both the topology and the layout of good routing trees. We address the class of *moment-matching* methods used to model distributed RLC interconnects with a small number of lumped segment models. We provide new *non-uniform* segment models which match the transfer function of a *general* interconnect line with source and load impedance up to second-degree terms. We also use this methodology to derive non-uniform lumped segment models for open-ended distributed RLC lines. Our approach can be used to derive compact, non-uniform equivalent circuits which match the distributed line transfer function to any given accuracy.

We have evaluated our models through simulation of interconnect networks by modeling the interconnect lines with *non-uniform* lumped segments and using the two-pole methodology. Although we use the two-pole method to demonstrate the advantage of our models and to reduce the complexity of simulation, the new models can be used within RLC model libraries for other circuit simulators such as SPICE. Previous two-pole approaches using traditional lumped segment models have over 25% error when compared to SPICE even for small interconnect tree examples. On the other hand, using our models the response becomes very close to the SPICE-computed response and delay estimates. For a wide range of interconnect parameters the delay estimates are all within 8% of SPICE-computed delays. As routing trees become bigger and interconnection lines become longer, particularly in MCM design, our approach has advantages in both accuracy and simulation complexity.

Finally, we show that computing the transfer function coefficients alone is enough to calculate the driving point admittance for interconnection trees. With this technique the two phase transfer function coefficient computation for interconnection trees in [26] can be reduced to "single phase", which reduces the computation time.

*This work was supported by NSF Young Investigator Award MIP-9257982.

1 Overview

Accurate calculation of propagation delay in VLSI interconnects is critical to the design of high speed systems. As feature sizes decrease and operating frequencies increase, interconnect delays come to dominate gate delays. Thus, interconnects are a major factor in the performance of high-speed integrated circuit, multichip and system-level designs. Direct simulation techniques such as SPICE give the most accurate insight into arbitrary interconnect structures, but are computationally expensive. Various techniques have been proposed for the simulation of interconnects [3, 28, 21, LK92], and most of these provide time-domain simulation methods. However, all of these methods are often very time consuming to estimate signal delay for even small network topologies. Especially when used during the design process of optimal design interconnects these methods become impractical. An effective and efficient way for delay estimation of interconnects is through moment matching techniques [17, 18, 27]. The output signal waveform can be approximated by first computing the moments and then applying the moment matching techniques. Asymptotic waveform evaluation (AWE) [18] uses moment computation method based on state variable approach (node voltages are recursively calculated by solving the circuit equations) for general RLC networks. RICE [20] extends AWE to handle transmission line tree structures for efficient simulation. But both AWE and RICE individual interconnects are modeled either using a large number of uniform RLC segments, which is neither exact nor efficient for interconnect simulation. Reciprocal expansion (REX) [26, 27] is based on two phase recursive admittance and transfer function coefficient computation. However, transmission lines are similarly modeled with several uniform segments. Faster techniques such as the two-pole approach [9, 34] have been used to calculate the response using the first and second moments but the these methods can be used only for delay computation and often result in inaccurate waveform estimation.

Traditionally, with these and previous approaches interconnects are modeled using uniform lumped RC and RLC segments. However, as interconnect lengths and operating frequencies increase, these simple lumped or "distributed-lumped" models can lead to errors, typically because only a few uniform lumped segments are computationally reasonable in modeling the interconnects, and because moments are not captured exactly.[1] A good review of lumped and distributed

[1] For example, Zhou et al. [34] calculate the response using an empirical relationship for the moment computation and approximate the off-path impedance as the sum of total subtree capacitance. This leads to an error in the second moment and the pole computation, which becomes significant as the size of off-path subtrees increases, as

RC models is given in [16, 6]). In this paper, we develop new segmented interconnect representations for delay simulation in interconnect trees; our goal is to improve both accuracy and efficiency over existing methodologies. Our work is aimed at the class of moment matching simulation approaches, which provide acceptable accuracy while maintaining computational efficiency. Traditionally, *uniform* lumped segment models (e.g., **L**, **T** or **Π** circuits) are used for modeling interconnect lines [9, 34]. With such representations, the moments are perfectly captured only as the number of segments used approaches infinity. With any finite number of segments, the moments will be either underestimated or overestimated depending on the type of segment (**L**, **T** or **Π**). The concept of *non-uniform* segment models is originally due to Rajput [19], who proposed a model with two non-uniform **L** segments to approximate the response of a distributed *RC* line. Rajput's equivalent circuit (i.e., lumped segment model) *exactly* matches the first two moments of the open-ended distributed *RC* line (i.e., up to the coefficient of s^2). Because the two non-uniform **L** segments achieve the exact accuracy that would require an infinite number of uniform **L** segments, simulation time is greatly reduced. Gerzberg [5] surveyed different non-uniform models and proposed a model in which the segment *RC* values are in geometric progression (the "Uniform Distributed *RC*" (URC) line model in SPICE is derived from Gerzberg's model).[2] The concept of non-uniform equivalent circuits has also been used in other areas, e.g., O'Brien et al. [14] and Gopal et al. [7] obtain non-uniform segment models for driving-point impedance at a gate output using moment-matching techniques. Recently Yu et al. [32] have also proposed a method, different from what we propose below, for deriving models by directly matching the moments of the transfer function. However, we note that their models are inaccurate as the complete set of constraints for the moment matching model are not considered.

We simulate interconnect trees using the non-uniform segment models and the two-pole methodology [9, 34].[3] However, we note that our models and techniques are not restricted to two pole and can be easily extended to any required accuracy. The response for higher order moments can be computed by converting the transfer function into a rational polynomial using *Padé* approximation. Previous two-pole approaches using traditional lumped segment models have sig-

in MCM interconnects.

[2]Sakurai [24] has observed that the use of a non-uniform equivalent circuit (i.e., lumped segment model) is not always appropriate since it cannot predict the correct response when the line is driven bidirectionally. However, in most routing tree design problems the direction of signal flow is known.

[3]While we use two-pole techniques for response calculations, the new segment models can be incorporated within *RLC* model libraries for other circuit simulators.

nificant error when compared to SPICE even for small interconnect tree examples, whereas using our models the response is typically quite close to the SPICE-computed response. For estimation of 90% threshold delay, our method is within 8% of the SPICE-computed delays for a wide range of interconnect parameter values and routing structures. Improvements in accuracy and simulation costs can be significant in the design of systems having large, high-speed interconnects.

Finally, we make a new interesting observation, and show that computing the transfer function coefficients alone is enough to calculate the driving point admittance for interconnection trees. With this technique the two phase transfer function coefficient computation for interconnection trees in [26, 27] can be reduced to "single phase" and reducing critical time complexity.

This paper is organized as follows. In Section 2 we provide basic concept of moments and the simple distributed 2-port model for transmission lines. Section 3 discusses various uniform segment models and their moment contribution to the transfer function. In Section 4, we propose new methodology to compute new accurate non-uniform k^{th} order RLC segment models for *general* transmission lines with source and load impedances. We also present *non-uniform* RC/RLC segment models for an open-ended distributed transmission line; these were originally reported in [10]. Section 5, we discuss general moment computation for interconnect trees and also general admittance computation at any subtree node. Since we use two-pole methodology for interconnect simulation, we present exact expressions for the first and second moments of the interconnect tree transfer function via a recursive expression for the admittance of a subtree which captures off-path subtree admittance accurately. In Section 6, we provide an interesting relationship between coefficients of the transfer function and driving point admittance, which reduces the transfer function coefficient computation method to a single pass algorithm. Finally, in Section 7 we present experimental results by simulate interconnect trees using the non-uniform segment models and the two-pole methodology [9, 34].

2 Basic Concepts for Interconnection Networks

2.1 Background on Moments

In a linear system, the transfer function $H(s) = \frac{V_{out}(s)}{V_{in}(s)}$ gives the relationship between the output response $V_{out}(s)$ and the input response $V_{in}(s)$. Let $h(t)$ be the impulse response corresponding

to the transfer function. Without loss of generality, the transfer function for any linear system can be expressed as a ratio of polynomials in s, that is to say,

$$H(s) = \frac{a_0 + a_1 s + a_2 s^2 + a_3 s^3 + ...}{b_0 + b_1 s + b_2 s^2 + b_3 s^3 + ...} \tag{1}$$

The i^{th} moment of the linear system is defined as

$$M_i = \frac{1}{i!}\int_0^\infty t^i h(t)dt = \frac{(-1)^i}{i!}H^{(i)}(0) \tag{2}$$

where $H^{(i)}(0)$ is the ith derivative of $H(s)$ at $s = 0$.

Assuming $v_{out}(0) = 0$, the Laplace transform of the derivative of the output voltage response for a unit step input is $v'_{out}(t) \Leftrightarrow sV_{out}(s) = s \cdot \frac{1}{s}H(s) = H(s) \Leftrightarrow h(t)$. Therefore, the transfer function can also be written as

$$H(s) = \int_0^\infty e^{-st} v'_{out}(t)dt.$$

Expanding e^{-st} into a Maclaurin series,

$$\begin{aligned} H(s) &= \int_0^\infty v'_{out}(t)dt - \frac{s}{1!}\int_0^\infty t v'_{out}(t)dt + \\ &\quad \frac{s^2}{2!}\int_0^\infty t^2 v'_{out}(t)dt - \frac{s^3}{3!}\int_0^\infty t^3 v'_{out}(t)dt + \ldots, \end{aligned}$$

and identifying the integral quantities as moments M_0, M_1, M_2, M_3 etc. from Equation (2), we get

$$H(s) = (M_0 - sM_1 + s^2 M_2 - s^3 M_3 + \ldots + (-1)^k M_k s^k + \ldots). \tag{3}$$

Therefore the moments can also be defined as

$$M_i = \frac{1}{i!}\int_0^\infty t^i v'_{out}(t)dt. \tag{4}$$

Observation 1: The relationship between transfer function moments and coefficients is given by

$$M_k = \frac{(-1)^{k+1}}{b_0}\sum_{i=1}^{k}(-1)^{k-i} b_i M_{k-i} + \frac{a_k}{b_0} \quad k \geq 1$$

Proof: Substituting for $H(s)$ in Equation (1) by the moment expansion given in (3), we have

$$(M_0 - M_1 s + M_2 s^2 - M_3 s^3 + \ldots + (-1)^k M_k s^k + \ldots) * (b_0 + b_1 s + b_2 s^2 + b_3 s^3 + \ldots) = (a_0 + a_1 s + a_2 s^2 + \ldots)$$

Matching the coefficients of s^k on both sides of the equation, we get

$$(-1)^k b_0 M_k + (-1)^{k-1} b_1 M_{k-1} + \ldots = a_k$$

from which

$$M_k = \frac{(-1)^{k+1}}{b_0} \sum_{i=1}^{k} (-1)^{k-i} b_i M_{k-i} + \frac{a_k}{b_0} \tag{5}$$

with

$$M_0 = \frac{a_0}{b_0}.$$

□

For the special case of a transfer function where the numerator polynomial is constant, i.e., $a_0 = 1$, $b_0 = 1$ ($M_0 = 1$), and $a_i = 0$ for $i \geq 1$, the relation between moments and coefficients is

$$M_k = (-1)^{k+1} \sum_{i=1}^{k} (-1)^{k-i} b_i M_{k-i} \quad \text{and} \quad b_k = -\sum_{i=1}^{k} (-1)^i M_i b_{k-i} \tag{6}$$

For further discussion of relationships between the moment representation and the time-domain response, see [17].

2.2 Moment Computation Through 2-port Analysis

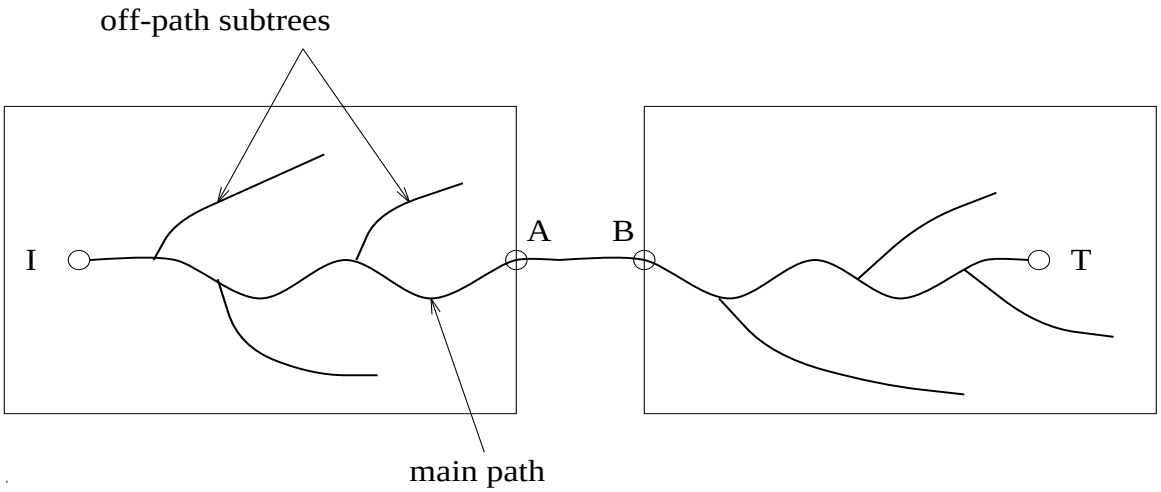

Figure 1: The *main path* of the routing tree between source I and load T.

For any RLC network, the coefficients a_i and b_i of the transfer function are in terms of R, L, C circuit parameters. Consider the interconnect line AB shown in the tree network of Figure 1. To model this interconnect line, we consider the source resistance and inductance, which are

respectively equal to the resistance and inductance of the main path from the source to the interconnect line. To simplify the analysis, we also approximate the load impedance by the total subtree capacitance at the end of the line; later, we remove this approximation and consider the total subtree admittance. The resulting representation of the interconnect line AB has source and load impedances as shown in Figure 2.

Definition: Let $Path(I,T)$ be the main path between the root node I and the leaf node T. Let C_N be the capacitance connected at node N and R_N, L_N be the resistance and inductance of the branch (or segment) between node N and its parent node $\hat{N}$. Also the son of node N on the main path is represented by $\check{N}$. $T(N)$ denotes the subtree rooted at the node N and $S(N)$ represents the set of son nodes of N.

The $ABCD$ parameters of the distributed RLC line portion of (Figure 2) are

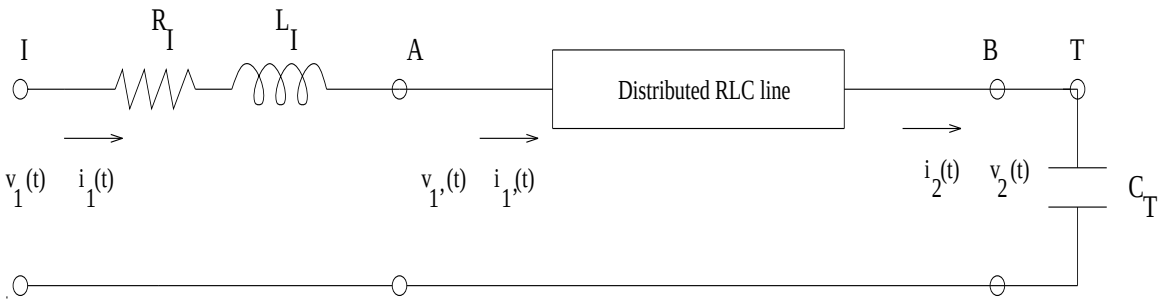

Figure 2: 2-port model of a distributed RLC line with source impedance $Z_I = R_I + sL_I$ and load impedance $Z_T = \frac{1}{sC_T}$.

$$\begin{pmatrix} V_A(s) \\ I_A(s) \end{pmatrix} = \begin{pmatrix} \cosh(\theta h) & Z_0 \sinh(\theta h) \\ \frac{1}{Z_0}\sinh(\theta h) & \cosh(\theta h) \end{pmatrix} \begin{pmatrix} V_B(s) \\ I_B(s) \end{pmatrix} \tag{7}$$

where $\theta = \sqrt{(r+sl)sc}$, h = length of the line, and $r = \frac{R}{h}$, $l = \frac{L}{h}$ and $c = \frac{C}{h}$ are the resistance, inductance and capacitance per unit length. $V_A(s), I_A(s)$ and $V_B(s), I_B(s)$ correspond to the voltage and current at, respectively, the left (input) port and right (output) port of the interconnect line respectively. The $ABCD$ parameters for entire section of the line including the source impedance are

$$\begin{pmatrix} V_I(s) \\ I_I(s) \end{pmatrix} = \begin{pmatrix} \cosh(\theta h) + \frac{Z_S}{Z_0}\sinh(\theta h) & Z_0 \sinh(\theta h) + Z_S \cosh(\theta h) \\ \frac{1}{Z_0}\sinh(\theta h) & \cosh(\theta h) \end{pmatrix} \begin{pmatrix} V_B(s) \\ I_B(s) \end{pmatrix} \tag{8}$$

Therefore, the transfer function between the nodes I and T is given by (see also [11]):

$$H(s) \;=\; \frac{V_B(s)}{V_I(s)} = \frac{1}{\cosh(\theta h)\left(1 + \frac{Z_I}{Z_T}\right) + \sinh(\theta h)\left(\frac{Z_I}{Z_0} + \frac{Z_0}{Z_T}\right)}$$

$$= \frac{1}{1 + sb_1^{IT} + s^2 b_2^{IT} + \ldots} \tag{9}$$

where $Z_T = \frac{1}{sC_T}$, $Z_I = R_I + sL_I$, $Z_0 = \sqrt{\frac{R+sL}{sC}}$ and $\theta h = \sqrt{(R+sL)sC}$. The first and second coefficients can be obtained as

$$\begin{aligned} b_1^{IT} &= R_I C + R_I C_T + \frac{RC}{2} + RC_T \\ b_2^{IT} &= \frac{R_I RC^2}{6} + \frac{R_I RCC_T}{2} + \frac{(RC)^2}{24} + \frac{R^2 CC_T}{6} + L_I C + L_I C_T + \frac{LC}{2} + LC_T \end{aligned} \tag{10}$$

For an open-ended distributed line with no source impedance, since $I_2(s) = 0$ the transfer function at the end of the line is given by

$$H(s) = \frac{1}{\cosh(\sqrt{(R+sL)sC})} = \frac{1}{1 + \frac{RC}{2}s + (\frac{(RC)^2}{24} + \frac{LC}{2})s^2 + (\frac{(RC)^3}{720} + \frac{RLC^2}{12})s^3 + ...} \tag{11}$$

Analogous results for the distributed RC line are obtained by substituting $L = 0$ in the above equation. We now present a recursive technique for calculating the coefficients of s of the transfer function for any general equivalent circuit; using this technique, the coefficients of the transfer function of the RLC line can also be computed.

3 Uniform Lumped Segment Models

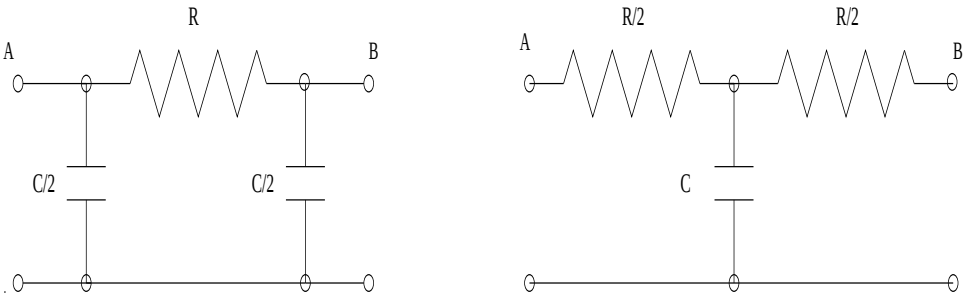

Figure 3: Elmore delay model - based on one segment **Π** and **T** model.

To model distributed RLC and RC lines, uniform **L**, **T** or **Π** models have traditionally been used. The accuracy of these models is highly dependent on the number of segments used for each distributed line. Sakurai [24] showed that for both the **T** and **Π** models, as the number of segments tends to infinity the equivalent circuit transfer function converges to the distributed RLC transfer function; [10] showed a similar result for the **L** segment model. Figures 4 and 3 show examples of uniform **L**, **T** and **Π** models, and Table 1 gives a comparison of the coefficients

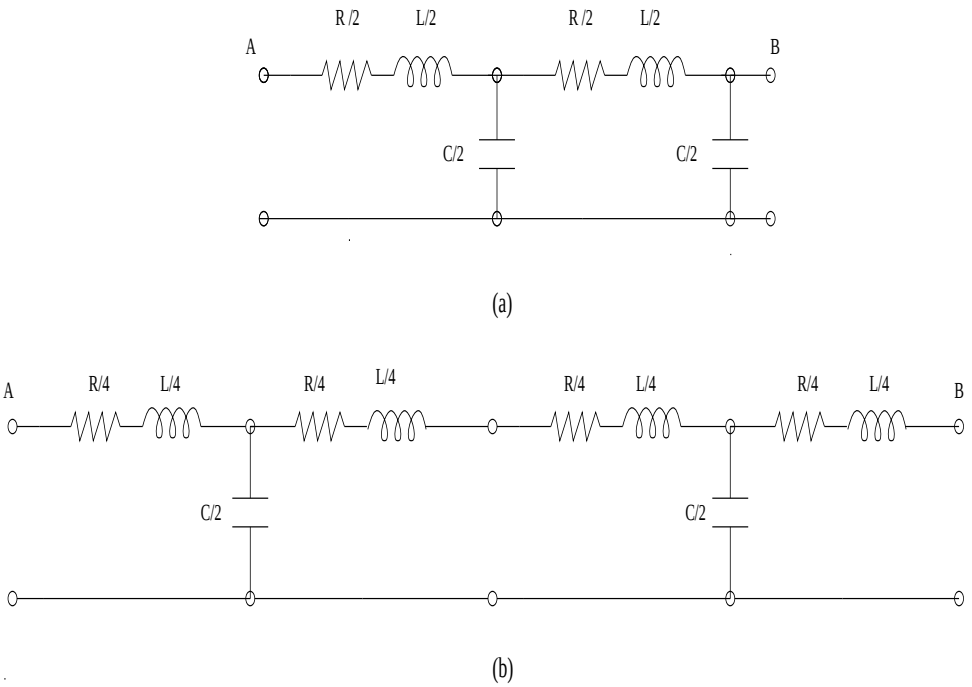

Figure 4: (a) Two uniform **L** and (b) two uniform **T** segments model for a distributed RC line.

	Method	b_1	b_2	b_3
1	Distributed RLC Line Model	$\frac{RC}{2}$	$\frac{(RC)^2}{24} + \frac{LC}{2}$	$\frac{(RC)^3}{720} + \frac{RLC^2}{12}$
2	Two uniform L segments	$\frac{3RC}{4}$	$\frac{(RC)^2}{16} + \frac{3LC}{4}$	$0 + \frac{RLC^2}{8}$
3	Three uniform L segments	$\frac{2RC}{3}$	$\frac{5(RC)^2}{81} + \frac{LC}{2}$	$\frac{(RC)^3}{729} + \frac{10RLC^2}{81}$
4	Two uniform T segments	$\frac{RC}{2}$	$\frac{(RC)^2}{32} + \frac{LC}{2}$	$0 + \frac{RLC^2}{16}$
5	Three uniform T segments	$\frac{RC}{2}$	$\frac{(RC)^2}{27} + \frac{LC}{2}$	$\frac{(RC)^3}{1458} + \frac{2RLC^2}{27}$
6	**Two non-uniform L segments**	$\frac{RC}{2}$	$\frac{(RC)^2}{24} + \frac{LC}{2}$	$0 + \frac{RLC^2}{12}$
7	**Three non-uniform L segments**	$\frac{RC}{2}$	$\frac{(RC)^2}{24} + \frac{LC}{2}$	$\frac{(RC)^3}{1111.11} + \frac{RLC^2}{12.02}$

Table 1: Various models approximating the open-ended transfer function of a distributed RLC line.

of various lumped models for small numbers of segments. Interestingly, with the uniform **L** model the convergence of the coefficient b_3 is not monotone with respect to the number of segments:

b_3 is close to its true value of 1/720 when there are three uniform segments, but then increases to its maximum error for seven segments before converging (see Figure 5). For example, using 10 uniform segments to approximate the behavior of a distributed RLC line entails error in the coefficient b_3 of around 25% (at the same time, the error in b_1 is around 10% and that of b_2 is 20%). The corresponding errors in the first moment and second moment are 10% and 20%, respectively. Since the voltage response is exponentially dependent on these moments, the resultant error in the response can be quite high. From the convergence of transfer function coefficients, we see that for any finite number of segments, the uniform **T** segments model **underestimates** the coefficient of s^2 in the denominator of the transfer function, while the uniform **L** segments model **overestimates** the coefficients of s and s^2.

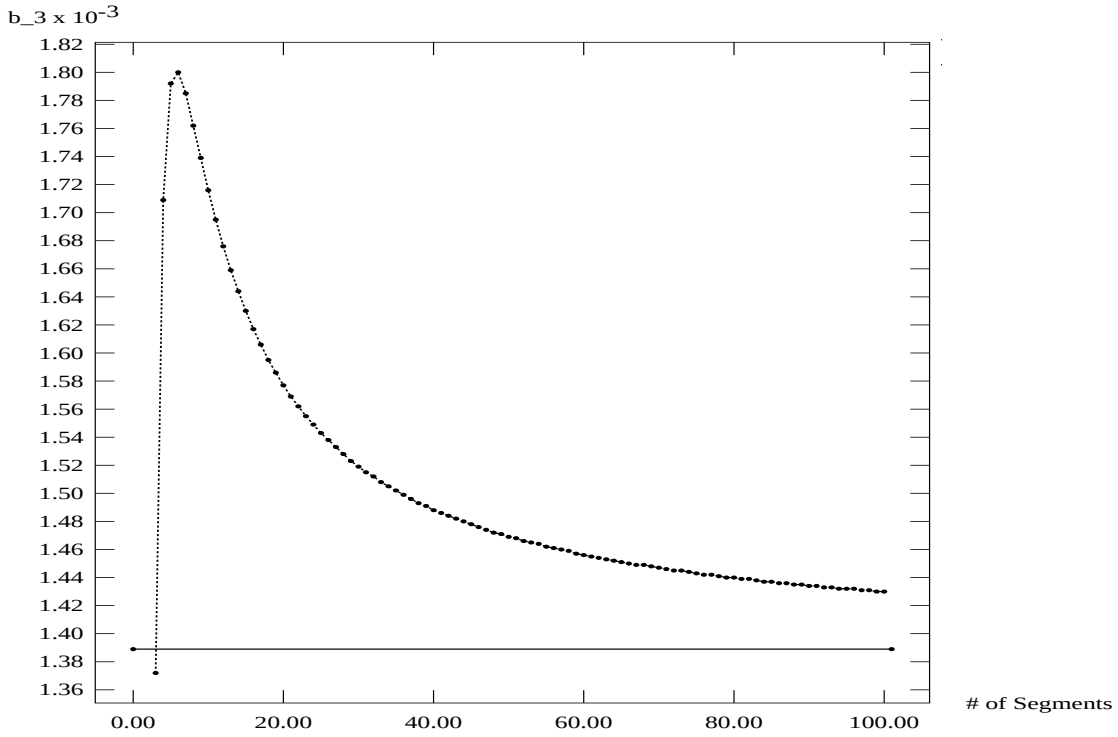

Figure 5: Convergence of b_3 (the coefficient of s^3) with respect to uniform **L** segments. The correct value of b_3 is 1/720 = 0.00139.

4 Non-Uniform Segment Models for General Interconnects

The aim of developing moment matching models for transmission line is to reduce the interconnection tree into the form of RLC or RLY tree. To make the computation of responses and

delay at the nodes efficient we would like to generate a moment model with minimum number of segments (or nodes) and still achieve good accuracy. The first order moment matching model consisting of one segment can easily derived and are shown in Figures 3. These models are often referred as "Elmore Delay" models. Rajput [19] derived an equivalent circuit (i.e., a lumped segment model) for the open-ended distributed RC line by matching both the transfer function and input impedance coefficients. The proposed equivalent circuit was composed of two non-uniform **L** segments. The circuit element values (refer to Figure 6) are given by

$$R_1 = \frac{1}{4}R, \qquad R_2 = \frac{3}{4}R$$
$$C_1 = \frac{2}{3}C, \qquad C_2 = \frac{1}{3}C$$

The coefficients corresponding to this equivalent circuit are given in Line 6 of Table 1 with inductance $L = 0$. Thus, the open-ended transfer function of a distributed RC line (Equation (11)) is captured **exactly** up to the coefficient of s^2, i.e., the first and second moments are exactly the same as for the distributed RC line. In [12] the calculation of non-uniform lumped models is extended to approximate the higher moments of the open-ended distributed RC line and to also obtain open-ended distributed RLC line models. In the remainder of this section, we develop the bases of out methodology for accurate interconnect tree analysis. First, we present a technique for calculating the coefficients b_k of the transfer function for any general equivalent circuit and for distributed lines. We then develop the appropriate non-uniform segment models for general interconnects.

4.1 Computation of Transfer Function Coefficients

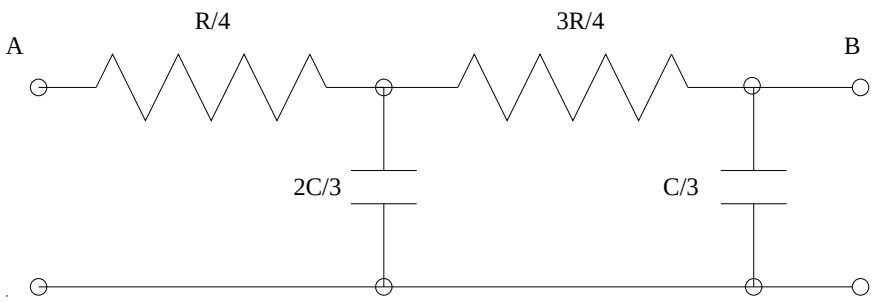

Figure 6: Two non-uniform **L** segment model for a distributed RC line.

Consider the general equivalent circuit consisting of N RLC segments as shown in Figure 7. Gao et al. [8] have given expressions for the coefficients of s and s^2 (i.e., b_1, and b_2); here we similarly

give a general expression for the coefficient of s^k [10].

Observation 2: Let b_k^i be the coefficient of s^k in the transfer function between node i and node 1. Then

$$b_k^{N+1} = R_N \sum_{j=1}^{N} C_j \cdot b_{k-1}^j + L_N \sum_{j=1}^{N} C_j \cdot b_{k-2}^j + b_k^N$$

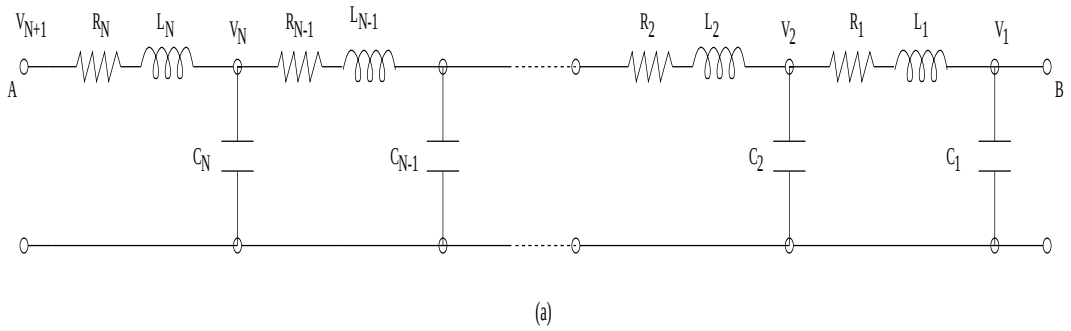

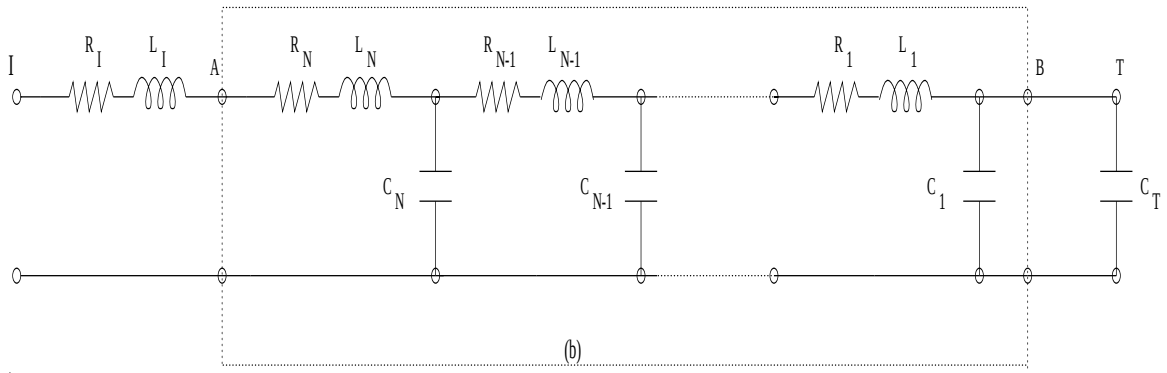

Figure 7: (a) N-segment RLC equivalent circuit for the distributed line, and (b) the N-segment line model with source and load impedance.

Proof: The voltage at node $N+1$ can be written using the recursive equation

$$\begin{aligned} V_{N+1}(s) &= (R_N + sL_N)\sum_{j=1}^{N} sC_j V_j(s) + V_N(s) \\ &= R_N(\sum_{j=1}^{N} sC_j V_j(s)) + sL_N(\sum_{j=1}^{N} sC_j V_j(s)) + V_N \end{aligned} \tag{12}$$

Expressing $V_{N+1}(s)$ as a series in s,

$$\frac{V_{N+1}(s)}{V_1(s)} = 1 + b_1^{N+1}s + b_2^{N+1}s^2 + b_3^{N+1}s^3 + ...$$

Replacing the node voltages in Equation (12) using this expression and collecting the terms for

coefficients of s^k, we get

$$b_k^{N+1} = R_N \sum_{j=1}^{N} C_j \cdot b_{k-1}^j + L_N \sum_{j=1}^{N} C_j \cdot b_{k-2}^j + b_k^N \tag{13}$$

□

We now use the above-described N-segment equivalent circuit to model the interconnect line AB of Figure 1. The source impedance of the path from the input source to the node A is represented by R_I and L_I. Similarly, the load impedance of the subtree rooted at the node B is represented by total subtree capacitance. From the recursion of Equation (13) the k^{th} coefficient of the transfer function between nodes I and T can be computed as

$$\begin{aligned} b_k^{IT} &= R_I \sum_{j=1}^{N} C_j b_{k-1}^j + L_I \sum_{j=1}^{N} C_j b_{k-2}^j + b_k^{(N+1)T} \\ &= R_I \sum_{j=1}^{N} C_j b_{k-1}^j + \sum_{j=1}^{N} C_j b_{k-1}^j \sum_{i=j}^{N} R_i + L_I \sum_{j=1}^{N} C_j b_{k-2}^j + \sum_{j=1}^{N} C_j b_{k-2}^j \sum_{i=j}^{N} L_i \end{aligned} \tag{14}$$

where $b_0^j = 1$ and $b_{-1}^j = 0$ for all j and for the special case of $k = 1$ the coefficients is

$$b_1^{IT} = R_I(\sum_{j=1}^{N} C_j + C_T) + \sum_{j=1}^{N} C_j \sum_{i=j}^{N} R_i + C_T \sum_{i=1}^{N} R_i \tag{15}$$

We will now give algorithm templates for computing transfer function coefficients based on Equation (13). We use the term $WC_k^N = \sum_{j=1}^{N} C_j b_{k-1}^j$ to represent the total k^{th} order "weighted capacitance" of the subtree rooted at node N. This term is recursively computed:

$$\begin{aligned} WC_k^N &= \sum_{j=1}^{N} C_j b_{k-1}^j \\ &= \sum_{j \in \mathcal{MP}(N,L)} C_j b_{k-1}^j \\ &= C_N b_{k-1}^N + \sum_{j \in \mathcal{MP}(\check{N},L)} C_j b_{k-1}^j \\ &= C_N b_{k-1}^N + WC_k^{\check{N}} \end{aligned} \tag{16}$$

Algorithm 1 gives the recursive weighted capacitance computation starting from the root node down to the target node. The weighted capacitance computation is the key to efficient computation of the transfer function coefficients. For any fixed moment order k, the complexity of Algorithm 1 is linear in the number of segments N in the main path. Algorithm 2 recursively

Algorithm 1: Weighted_Capacitance(N,k)
Input: $\mathcal{T}(N) \equiv$ interconnection tree $k \equiv$ required moment order
Output: $WC(N,k)$, i.e., WC_k^N
$WC(N,k) = C_N b_{k-1}^N$ if N is not a leaf node $WC(N,k) = WC(N,k)+$ Weighted_Capacitance($\check{N}$, k) store($WC(N,k)$) return

Algorithm 2: Transfer_Coefficient(N,k)
Input: $\mathcal{T}(N) \equiv$ interconnection tree $\mathcal{MP}(N,L) \equiv$ main path from source N to target L $k \equiv$ required moment order $b(N,j) \equiv$ previous transfer function coefficient (for $j = 1$ to $k-1$)
Output: $b(N,k) \equiv$ transfer function coefficient b_k^N
Weighted_Capacitance(N,k) if N is a leaf node if $k \geq 1$ then $b(N,k) = 0$ if $k = 0$ then $b(N,k) = 1$ else $b(N,k) = b(N,k)+$ Transfer_Coefficient($\check{N},k$) $+R_N WC(N,k-1) + L_N WC(N,k-2)$ store($b(N,k)$) return

computes transfer function coefficients based on the weighted capacitance computation. The complexity of Algorithm 2 is also linear in the number of segments N in the main path.

Observation 3: For uniform segment values with $R_j = \frac{R}{N}$, $L_j = \frac{L}{N}$ and $C_j = \frac{C}{N}$, the transfer function coefficients from Equation (14) will reduce to those in Equation (10) in the limit as $N \to \infty$.

Proof: By induction.

Substituting $R_j = \frac{R}{N}$, $L_j = \frac{L}{N}$ and $C_j = \frac{C}{N}$ in Equation (15) we get

$$b_1^{IT} = R_I(C + C_T) + \sum_{j=1}^{N} \frac{RC}{N^2}(N - j + 1) + RC_T$$

and in the limit as $N \rightarrow \infty$,

$$b_1^{IT} = R_I(C + C_T) + \frac{RC}{2} + RC_T$$

From Equation (14), we have

$$\begin{aligned} b_2^{IT} &= R_I \sum_{j=1}^{N} C_j b_1^j + \sum_{j=1}^{N} C_j b_1^j \sum_{i=j}^{N} R_i \\ &\quad + L_I(\sum_{j=1}^{N} C_j + C_T) + \sum_{j=1}^{N} C_j \sum_{i=j}^{N} L_i + C_T \sum_{i=1}^{N} L_i \\ &= R_I \frac{C}{N} \sum_{j=1}^{N} b_1^j + \frac{RC}{N^2} \sum_{j=1}^{N} b_1^j (N - j + 1) \\ &\quad + L_I(C + C_T) + \sum_{j=1}^{N} \frac{LC}{N^2}(N - j + 1) + LC_T \end{aligned} \tag{17}$$

Substituting for b_1^j from the recursive computation as

$$b_1^j = \frac{RC_T(j-1)}{N} + \frac{RCj(j-1)}{2N^2}$$

and taking the limit as $N \rightarrow \infty$, we obtain

$$\lim_{N\to\infty} \frac{1}{N} \sum_{j=1}^{N} b_1^j = \frac{RC_T}{2} + \frac{RC}{6} \qquad \text{and} \qquad \lim_{N\to\infty} \frac{1}{N^2} \sum_{j=1}^{N} j b_1^j = \frac{RC_T}{3} + \frac{RC}{8}$$

Therefore,

$$b_2^{IT} = \frac{R_I RC^2}{6} + \frac{R_I RCC_T}{2} + \frac{(RC)^2}{24} + \frac{R^2 CC_T}{6} + L_I C + L_I C_T + \frac{LC}{2} + LC_T$$

The convergence of other coefficients can be similarly proved. □

4.2 Computation of Non-uniform Models

We may obtain non-uniform equivalent circuit models for a distributed line with general source and load impedances by computing the coefficients using Equation (14) and matching with the distributed transfer function coefficients given by Equation (10).

Observation 4: For any non-uniform RLC equivalent circuit model, the resistances and inductances are identically distributed, i.e.,

$$R_i = L_i \qquad \forall\ i.$$

Proof: The constraints obtained for inductance parameters using the Equation (14) for b_k are of the form $\sum_{j=1}^{N} C_j b_{k-2}^j$, which are identical to constraints for resistive parameters according to the b_{k-1} equation. The resistive parameters will have extra constraints from b_k equation, but in the limit of large k the constraints on inductive elements are the same as the constraints on resistive elements. Therefore, $R_i = L_i \qquad \forall\ i$. □

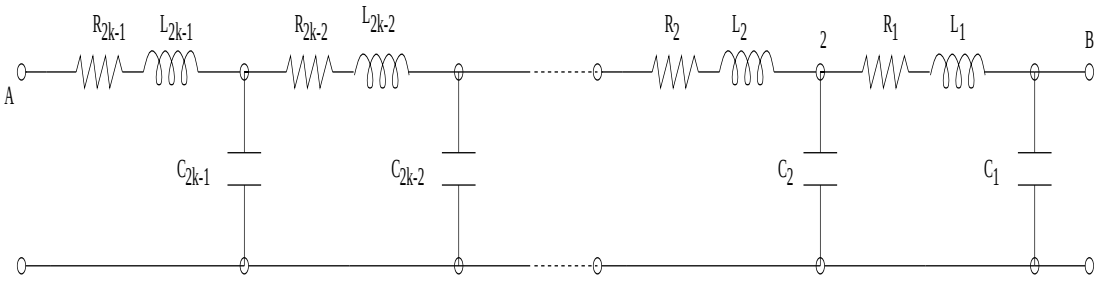

(a)

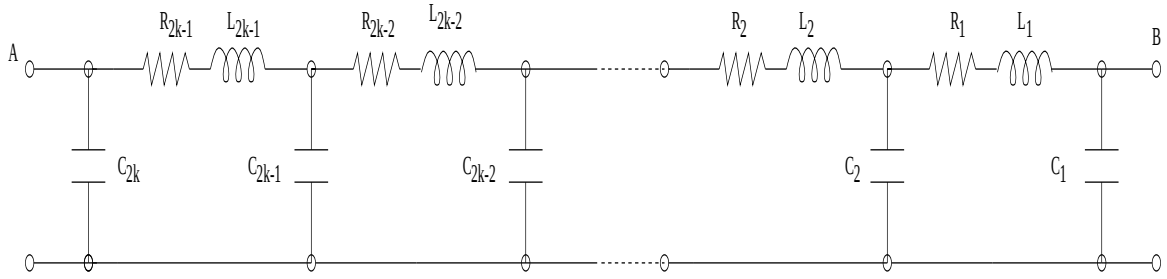

(b)

Figure 8: k^{th} moment matching **L** and **Π** segment models.

Therefore, we need derive constraints only for resistance and capacitance parameters of the equivalent circuit. The constraints required to solve for calculating the parameters of the moment matching model can be obtained by matching the transfer function coefficients of the model and the corresponding distributed line model. In general the k^{th} coefficient of the transfer function of a r segment equivalent circuit can be obtained directly from Equation (14)

$$b_k = R_I \sum_{j=1}^{r} C_j b_{k-1}^j + \sum_{j=1}^{r} C_j b_{k-1}^j \sum_{i=j}^{r} R_i + L_I \sum_{j=1}^{r} C_j b_{k-2}^j + \sum_{j=1}^{r} C_j b_{k-2}^j \sum_{i=j}^{r} L_i \qquad (18)$$

Figure 8 shows k^{th} moment matching model using **L** and **Π** segment models. Similarly, the transfer function coefficients for the distributed RLC can be obtained by considering uniform segment values with number of segments tending to infinity. This was proved for the first few

coefficients in the **Observation 2**. From Equation (18), we see that there are two terms which generate the constraints (not considering inductance terms). Therefore, the constraints required to obtain k^{th} order moment matching model with r segments are:

$$\begin{aligned} \sum_{i=1}^{r} R_i &= R \\ \sum_{i=1}^{r} C_i b_{j-1}^i &= \lim_{N\to\infty} \frac{C}{N} \sum_{i=1}^{N} b_{j-1}^i \\ \sum_{i=1}^{r} C_i b_{j-1}^i \sum_{l=i}^{r} R_l &= \lim_{N\to\infty} \frac{RC}{N^2} \sum_{i=1}^{N} (N-i+1) b_{j-1}^i \end{aligned} \tag{19}$$

where $j = 1, 2, \ldots k$. The constraint for total capacitance is obtained from the second equation set with $j = 1$. It is easy to see that the number of constraints from the above set are $2k + 1$ for k^{th} moment model. But each constraint set further can divided into two classes: one which considers the current drawn at the load (i.e., with capacitive load term C_T) and second with current drawn from the model itself. Actually the direct dependence on the C_T term can be seen for b_1 in Equation (15) and higher coefficients the dependence is implicit. Therefore, there are four different terms with resistance and capacitance values in each coefficient of s^k. The four different terms can be easily identified for b_2 of the distributed line in **Observation 2**.[4] These are the source resistance (R_I) term, the source resistance and load capacitance ($R_I C_T$) term, the line resistance and capacitance (RC) term, and the line resistance and load capacitance (RC_T) term. However, the source resistance and load capacitance ($R_I C_T$) term in the coefficient of s does not yield any constraints, so there are a total of $4k - 1$ constraints in matching up to k coefficients in the equivalent circuit.

Therefore, by using $2k - 1$ **Π** segments we can exactly match the total $4k - 1$ constraints. Also $2k - 1$ **L** segments equivalent circuit can be used but will generate overspecified system of equations [13]. Here, we note that the constraints generated using Yu and Kuh's method [32] are not complete, as they do not consider the constraints corresponding to the load term are not considered. We note that this could be the reason for the different model parameters in the second order moment matching model (see Figure 9). So it can be concluded that open-ended models derived should be same as those proposed in [32] as there are no constraints from the load term. This conclusion can be verified by observation our both second order and third order open-ened models (see Appendix C).

[4] Appendix B and Appendix C discuss in more detail the constraints formed for three segment models.

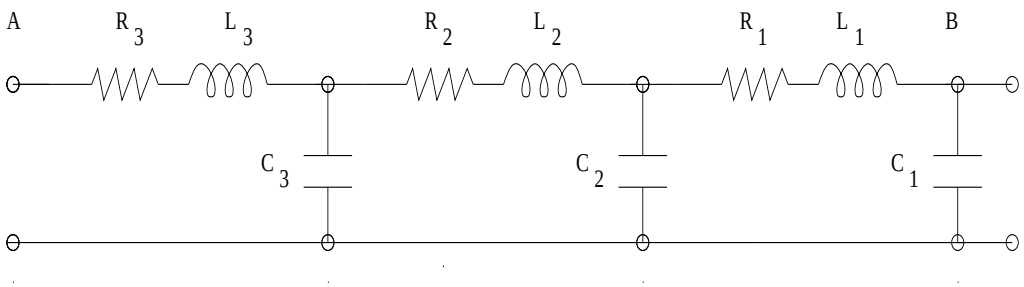

(a)

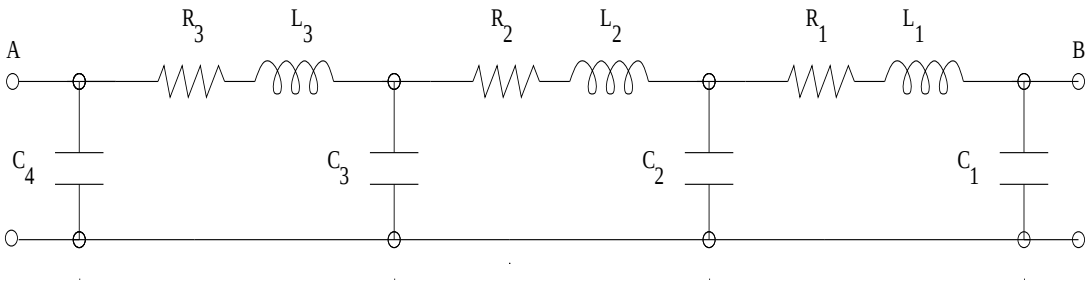

(b)

Figure 9: Non-uniform three **L** and **Π** segment model for a general distributed RLC line.

Example: To illustrate the method, here we give third order moment matching model. In particular, to derive equivalent circuits which match up to the coefficient of s^2 we need to satisfy 7 constraints; this can be achieved by using 3 **L** or **Π** segments. We use numerical search to solve for the equivalent circuit parameters. The equivalent **L** circuit parameters (Figure 9) for matching up to the second moment are given by

$$R_1 = 0.40R, \qquad R_2 = 0.40R, \qquad R_3 = 0.20R$$

$$L_1 = 0.40L, \qquad L_2 = 0.40L, \qquad L_3 = 0.20L$$

$$C_1 = 0.17C, \qquad C_2 = 0.41C, \qquad C_3 = 0.42C \tag{20}$$

Similarly, the equivalent **Π** circuit parameters (Figure 9) are obtained as

$$R_1 = 0.34R, \qquad R_2 = 0.32R, \qquad R_3 = 0.34R$$

$$L_1 = 0.34L, \qquad L_2 = 0.32L, \qquad L_3 = 0.34L$$

$$C_1 = 0.15C \qquad C_2 = 0.35C, \qquad C_3 = 0.35C \qquad C_4 = 0.15C \tag{21}$$

Note that the **Π** circuit parameters are symmetrical, in contrast to the **L** circuit model.

Finally, we develop models for a distributed open-ended line with no source impedance, a case which has received wide interest in the [19, 5, 10]. With no source and load impedance the transfer function coefficients in Equation (14) will reduce to only one term, i.e.,

$$b_k^{IT} = \sum_{j=1}^{N} C_j b_{k-1}^j \sum_{i=j}^{N} R_i + \sum_{j=1}^{N} C_j b_{k-2}^j \sum_{i=j}^{N} L_i \tag{22}$$

which results in k constraints to match up to k coefficients of the open-ended transfer function. As before, by matching the first k coefficients of the input impedance, another k constraints can be obtained. The resulting $2k$ constraints can be satisfied by using k non-uniform **L** segment models. Therefore, to match up to the coefficient of s^3 in the open-ended transfer function we need only three **L** segments, as compared to five **L** segments in the case of a general distributed line with source and load impedance. For comparison, note that the three non-uniform segment model with open-ended assumption has the following parameters[5] [12] (see Appendix C)

$$R_1 = 0.50R, \qquad R_2 = 0.20R, \qquad R_3 = 0.30R$$

$$L_1 = 0.50L, \qquad L_2 = 0.20L, \qquad L_3 = 0.30L$$

$$C_1 = 0.16C, \qquad C_2 = 0.44C, \qquad C_3 = 0.40C$$

The non-uniform equivalent circuits that we have developed can also be employed in place of the lumped **T** and **Π** models that are traditionally used for clock skew minimization and other performance-driven routing applications.

5 Interconnect Tree Analysis

Various methods have been proposed for calculating the response and delay of interconnect trees. The simplest and most widely used method is to estimate the delay using the Elmore delay model [4], i.e., a single-pole approximation of the transfer function. To obtain the delay estimates for interconnect trees, Rubinstein et al. [22] defined a main path between the source and sink of interest. Using the Elmore delay expression for RC trees [22], the following delay model for

[5] The coefficients corresponding to non-uniform model of open-ended line are given in Line 7 of Table 1.

interconnect trees was developed:

$$T_{ED} = R_0 C_{T(S)} + \sum_{\forall i \in M(S,T)} R_i (\frac{C_i}{2} + C_{T(i)})$$

where $T(S)$ is the tree rooted at source S, $T(i)$ is the subtree rooted at node i, and $M(S,T)$ is the main path between source S and the sink T. While this model is widely used for interconnect tree analysis and synthesis, its disadvantages are that it is a single-pole approximation and that it does not take into account the inductance of the interconnect line. Since inductance becomes more significant as feature sizes decrease, layout dimensions increase, and operating frequencies increase, interconnect trees which minimize Elmore delay can be sub-optimal.

Methods which calculate more than one dominant pole from the moments of the transfer function will lead to improved delay estimates. Previous two-pole methods [9, 8, 34] calculate the two dominant poles of the transfer function from the first and second moments by modeling each distributed line separately with uniform lumped segment models (ladders of **L**, **T** or **Π** circuits). As noted earlier, for such uniform representations the moments are perfectly captured only as the number of segments used approaches infinity, which is computationally unreasonable. Thus, we propose to use the non-uniform models derived in Section 4, which match the transfer function exactly up to the coefficient of s^2. Another drawback of previous two-pole methods [9, 8, 34] is that the off-path subtree admittance is approximated by the total subtree capacitance; this provides a correct approximation only up to the coefficient of s in the subtree admittance.[6] Thus, we propose a method to obtain the coefficients of the transfer function *exactly* by considering the off-path subtree admittance. We now describe our approach for calculating the response at a given sink of a general interconnection tree. We first derive exact expressions for the first and second moments in terms of the lumped segment parameters used to model the distributed lines.

5.1 Tree Moment Computations

Consider the *main path* between the source and sink of interest, and replace each subtree by its respective admittance. To calculate the response at the sink we use an approach similar to that of Gao et al. [8]. Figure 10 shows an example of a main path where each branch in the tree is replaced by a single RLC segment, and subtrees are replaced by their respective admittances.

[6] Also, Zhou et al. [34] used a special polynomial function that describes the poles by heuristically incorporating a model proposed by [33], instead of using the standard two-pole methodology (Appendix A).

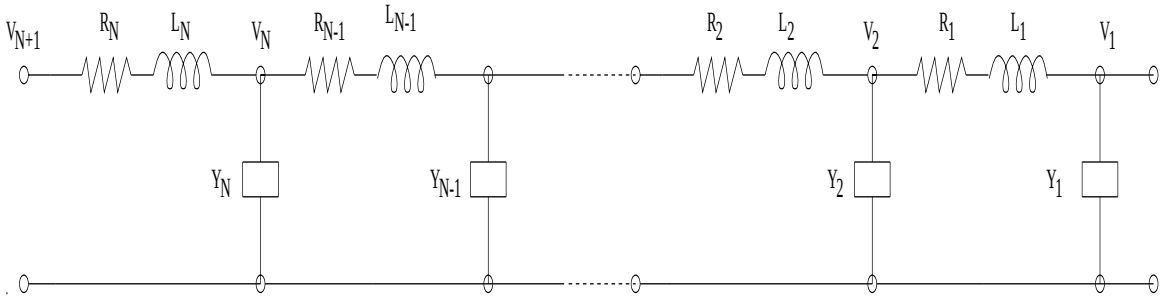

Figure 10: Representation of the main path in the tree, where each distributed line is modeled using RLC segments. Y_i indicates the off-path subtree admittance at node i.

The node V_{N+1} indicates the source, and V_1 indicates the sink of interest. At any node i, the admittance Y_i is equal to (i) the capacitance of node i if there is no subtree at node i, or (ii) to the sum of the subtree admittance and the admittance of the capacitance of the equivalent circuit, otherwise. In other words,

$$\begin{aligned} Y_i &= sC_i && \text{if node } i \text{ has no off-path subtree} \\ &= sC_i + Y_{T(i)} && \text{if node } i \text{ has off-path subtree} \end{aligned}$$

Observation 5: Let b_k^i be the coefficient of s^k in the transfer function of the main path between node i and node 1. Then in Figure 10

$$b_k^{N+1} = R_N \sum_{l=1}^{k} \sum_{j=1}^{N} Y_{l,j} b_{k-l}^j + L_N \sum_{l=1}^{k-1} \sum_{j=1}^{N} Y_{l,j} b_{k-1-l}^j + b_k^N$$

Proof: The input voltage for the main path in Figure 10 can be written as

$$V_{N+1}(s) = (R_N + sL_N)(\sum_{j=1}^{N} Y_j(s) V_j(s)) + V_N(s)$$

where $Y_j(s) = sY_{1,j} + s^2 Y_{2,j} + \ldots$ with $Y_{1,j}$ and $Y_{2,j}$ being the coefficients of s and s^2 of the subtree admittance. Expressing $V_{N+1}(s)$ as a series expansion of s, $V_{N+1}(s) = V_1(s)(1 + b_1^{N+1} s + b_2^{N+1} s^2 + b_3^{N+1} s^3 + ...)$. The general expression for the transfer function coefficient of s^k is

$$b_k^{N+1} = R_N \sum_{l=1}^{k} \sum_{j=1}^{N} Y_{l,j} b_{k-l}^j + L_N \sum_{l=1}^{k-1} \sum_{j=1}^{N} Y_{l,j} b_{k-1-l}^j + b_k^N \tag{23}$$

□

Using this recursive equation, the k^{th} coefficient of the transfer function can be obtained as

$$b_k^{N+1} = \sum_{l=1}^{k} \sum_{j=1}^{N} Y_{l,j} b_{k-l}^j \sum_{i=j}^{N} R_i + \sum_{l=1}^{k-1} \sum_{j=1}^{N} Y_{l,j} b_{k-1-l}^j \sum_{i=j}^{N} R_i \tag{24}$$

The term $\sum_{l=1}^{k}\sum_{j=1}^{N} Y_{l,j}b_{k-l}^{j}$ is the total k^{th} order "weighted admittance" WY_k^N of the subtree rooted at node N, and can be written recursively as

$$\begin{aligned} WY_k^N &= \sum_{l=1}^{k}\sum_{j\in T(N)} Y_{l,j}b_{k-l}^{j} = \sum_{l=1}^{k} Y_{l,N}b_{k-l}^{N} + \sum_{l=1}^{k}\sum_{j\in T(N-1)} Y_{l,j}b_{k-l}^{j} \\ &= \sum_{l=1}^{k} Y_{l,N}b_{k-l}^{N} + WY_k^{N-1} \end{aligned} \tag{25}$$

Algorithm 3 recursively computes the weighted admittance from the root node down to the target node. Algorithm 4 gives the transfer function coefficient computation, which is very similar to that for the RLC tree except for the weighted admittance. The only unknown parameters at this stage are the admittance computation at each node of the interconnection tree.

Algorithm 3: Weighted_Admittance(N, k)

Input: Interconnection Tree $\mathcal{T}(S) \equiv$ interconnection tree
$k \equiv$ required moment order
$Y_i \equiv$ admittance for all nodes i

Output: $WY(N,k)$

$WY(N,k) = \sum_{l=1}^{k} Y_{l,N}b_{k-l}^{N}$
if N is not a leaf node
  $WY(N,k) = WY(N,k)$+ Weighted_Admittance($\check{N}$, k)
store($WY(N,k)$)
return

Algorithm 4: Transfer_Coefficient(N,k)

Input: $\mathcal{T}(N)equiv$ interconnection tree
$\mathcal{MP}(N,L) \equiv$ main path from node N to target L
$k \equiv$ required moment order
$b(N,j) \equiv$ previous transfer function coefficient (for $j = 1$ to $k-1$)

Output: $b(N,k) \equiv$ transfer function coefficient $b(N,j)$

Weighted_Admittance(N,k)
if N is a leaf node
  if $k \geq 1$ then $b(N,k) = 0$
  if $k = 1$ then $b(N,k) = 1$
else
  $b(N,k) = b(N,k)$+ Transfer_Coefficient($\check{N},k$)
  $+R_N WY(N,k-1) + L_N WY(N,k-2)$
store($b(N,k)$)
return

Example: Using the above recursive equation the expressions for the first and second coefficients

of the transfer function. can be derived as

$$\begin{aligned} b_1^{N+1} &= R_N \sum_{j=1}^{N} Y_{1,j} + b_1^N = \sum_{i=1}^{N} R_i \sum_{j=1}^{i} Y_{1,j} = \sum_{j=1}^{N} Y_{1,j} \sum_{i=j}^{N} R_i \\ b_2^{N+1} &= R_N \sum_{j=1}^{N} Y_{1,j} b_1^j + R_N \sum_{j=1}^{N} Y_{2,j} + L_N \sum_{j=1}^{N} Y_{1,j} + b_2^N \\ &= \sum_{j=2}^{N} Y_{1,j} \sum_{l=j}^{N} R_l \sum_{i=1}^{j-1} Y_{1,i} \sum_{d=i}^{j-1} R_d + \sum_{j=1}^{N} Y_{2,j} \sum_{l=j}^{N} R_l + \sum_{j=1}^{N} Y_{1,j} \sum_{l=j}^{N} L_l \end{aligned}$$

We thus obtain a general expression for coefficients of the transfer function in terms of parameters of the main path and the subtree admittance coefficients. The moments of the transfer function can be calculated from the transfer function coefficients using the recursive Equation (6)

$$M_k = (-1)^{k+1} \sum_{i=1}^{k} (-1)^{k-i} b_i M_{k-i}$$

so that the first and second moments are given by:

$$\begin{aligned} M_1 &= b_1 = -\sum_{j=1}^{N} Y_{1,j} \sum_{i=j}^{N} R_i \\ M_2 &= b_1^2 - b_2 = (\sum_{j=1}^{N} Y_{1,j} \sum_{i=j}^{N} R_i)^2 - \sum_{j=1}^{N} Y_{2,j} \sum_{l=j}^{N} R_l \\ &\quad - \sum_{j=2}^{N} Y_j^1 \sum_{l=j}^{N} R_l \sum_{i=1}^{j-1} Y_i^1 \sum_{d=i}^{j-1} R_d - \sum_{j=1}^{N} C_j \sum_{l=j}^{N} L_l \end{aligned} \tag{26}$$

5.2 Computation of Subtree Admittance

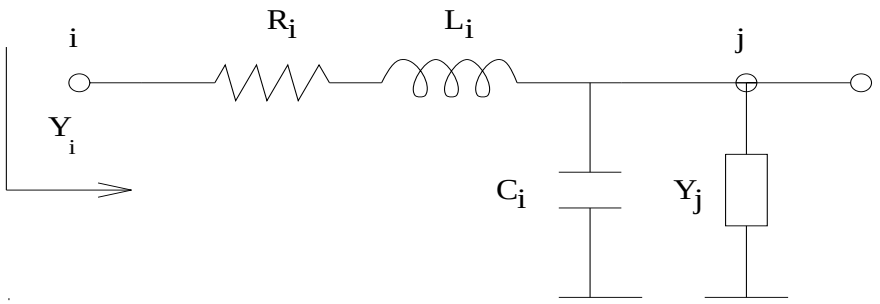

Figure 11: A single RLC segment between nodes i and j.

In this subsection, we analyze the computation of admittance coefficients and give a recursive expression for the k^{th} admittance coefficient. For computation of the first and second moments

of the interconnect tree, we then derive the coefficients s and s^2 ($Y_{1,i}$ and $Y_{2,i}$) of the subtree admittance.

Observation 6: The admittance at node i in Figure 11 can be computed recursively in terms of admittance at node j as:

$$Y_{1,i} = Y_{1,j} + C_i$$

and

$$Y_{k,i} = Y_{k,j} - R_i \sum_{l=1}^{k-1} Y_{l,i} Y_{k-l,j} - L_i \sum_{l=1}^{k-2} Y_{l,i} Y_{k-1-l,j} - R_i C_i Y_{k-1,i} - L_i C_i Y_{k-2,i} \quad \text{for } k \geq 2$$

Proof: Consider a single section of a subtree where Y_j in the Figure 11 indicates the admittance of the subtree rooted at node j. In general, the admittance at node i can be expressed in terms of the admittance at node j as

$$\begin{aligned} Y_i &= \frac{1}{R_i + sL_i + \frac{1}{(Y_j + sC_i)}} \\ &= \frac{(Y_j + sC_i)}{1 + (R_i + sL_i)(Y_j + sC_i)} \end{aligned}$$

Rearranging the above equation, we get

$$Y_i + R_i Y_i Y_j + sL_i Y_i Y_j + sR_i C_i Y_i + s^2 L_i C_i Y_i = Y_j + sC_i$$

Substituting for admittance Y_j as a polynomial in s, $Y_j(s) = sY_{1,j} + s^2 Y_{2,j} + \ldots$ and for Y_i with $Y_i(s) = sY_{1,i} + s^2 Y_{2,i} + \ldots$, where $Y_0 = 0$, we get

$$Y_{1,i} = Y_{1,j} + C_i$$

and the k^{th} coefficient ($k \geq 2$) of admittance is

$$Y_{k,i} = Y_{k,j} - R_i \sum_{l=1}^{k-1} Y_{l,i} Y_{k-l,j} - L_i \sum_{l=1}^{k-2} Y_{l,i} Y_{k-1-l,j} - R_i C_i Y_{k-1,i} - L_i C_i Y_{k-2,i} \qquad (27)$$

□

From the recursive equation (27) the coefficient of s^2 of the admittance at node i is given by

$$\begin{aligned} Y_{2,i} &= Y_{2,j} - R_i Y_{1,i} Y_{1,j} - R_i C_i Y_{1,i} \\ &= Y_{2,j} - R_i (Y_{1,j} + C_i)^2 \end{aligned}$$

By substitution, the admittance coefficients s and s^2 for N RLC segments connected in series (Figure 7) are given by

$$\begin{aligned} Y_{1,N+1} &= \sum_{j=1}^{N} C_j \\ Y_{2,N+1} &= -\sum_{i=1}^{N} R_i (\sum_{j \in T(i)} C_j)^2 \end{aligned} \tag{28}$$

where we use $T(i)$ to denote the set of nodes in the subtree rooted at node i. Equation (28) yields the coefficients of s and s^2 of the admittance, which are then used in the first and second moment calculations in Equation (26). We note that analysis of admittance computation, for the first few coefficients only, has also been discussed in [14, 15, 25].

Example: A Simple Interconnection Tree. We now derive the first and second moments for the transfer function of a simple interconnection tree with node 1 as source and node 3 as the sink of interest as shown in Figure 12. For simplicity, we use a single RLC segment shown in Figure 11 to model each edge of the interconnect tree. However, in practice accurate segment models (e.g., non-uniform segment models [12, 13] or models which have many traditional uniform **L**, **T** or **Π** segments) are more likely to be used.

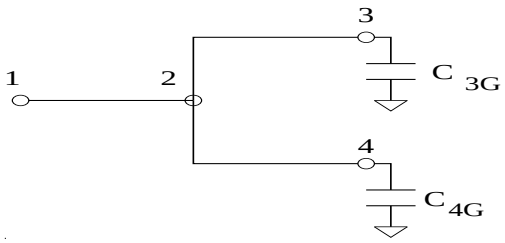

Figure 12: An example of an interconnection tree.

We now compute the coefficients of the transfer function for the main path between nodes 1 and 3. The subtree at node 2 will be replaced by its corresponding admittance, whose moments are computed using the methodology described above. The admittance moments for the subtree at node 2 are:

$$\begin{aligned} Y_{1,2} &= C_{24} + C_{4G} \\ Y_{2,2} &= -R_{24}(C_{24} + C_{4G})^2 \end{aligned}$$

The first moments of the transfer function at various nodes in the main path are

$$\begin{aligned} b_1^3 &= 0 \\ b_1^2 &= R_{23}Y_{1,3} = R_{23}(C_{23} + C_{3G}) \\ b_1^1 &= R_{12}Y_{1,2} + b_1^2 = R_{12}(C_{12} + C_{23} + C_{24} + C_{3G} + C_{4G}) \end{aligned}$$

and the second moments of the transfer function are

$$\begin{aligned} b_2^3 &= 0 \\ b_2^2 &= L_{23}Y_{1,3} = L_{23}(C_{23} + C_{3G}) \\ b_2^1 &= R_{12} \cdot (C_{12} + Y_{1,2})b_1^2 + R_{12} \cdot Y_{2,2} + L_{23} \cdot (C_{12} + Y_{1,2} + Y_{1,3}) + b_2^2 \\ &= R_{12}R_{23}((C_{12} + C_{24} + C_{4G})(C_{23} + C_{3G}) - R_{12}R_{24}(C_{24} + C_{4G})^2 \\ &\quad + L_{23}(C_{12} + C_{24} + C_{4G} + C_{23} + C_{3G}) + L_{23}(C_{23} + C_{3G}) \end{aligned}$$

5.3 Time Complexity

For large routing trees, using non-uniform equivalent circuits to represent distributed RLC lines will reduce the computation time significantly compared to using a number of uniform RLC segments. Previous works such as [22, 34, 27] suggest using m uniform segments to model each interconnect line (for instance, [2] divides each line into $25\mu m$ segments and then models each segment using a uniform **L** type RLC circuit); m could be quite large for MCM substrate or other global system-level interconnects. Let N be the total number of interconnect lines from the input node to the output node (i.e., on the main path). The computation time for calculating k admittance coefficients via Equation (27) for all the interconnect nodes is $O(mNk^2)$. The computation time for coefficient b_k from Equation (23) is $O(m^2N^2k^2)$. Using non-uniform models with few segments the computation time for admittance will be reduced to $O(Nk^2)$, and the computation time for coefficient b_k will be reduced to $O(N^2k^2)$; this speedup will be significant if the interconnection tree is large or if accuracy is desired.[7] Similarly, by approximating the subtree admittance by the total subtree capacitance the computation time for coefficient b_k from Equation (23) is $O(m^2N^2k)$, which again reduces to $O(N^2k)$ for interconnect simulation with new model.

[7] With 10 uniform segments, the errors in the first and second moments are 10% and 20%; even with 25 uniform segments these errors are still 5% and 8% [10].

6 Computation of Driving Point Admittance Coefficients

Previously, we have concentrated on computing coefficients of models for the transfer function of distributed interconnect lines. We now extend the discussion to compute the coefficients of the driving point admittance (or impedance) function. From this, we will be able to derive a simple single **Π** segment equivalent model to represent the driving point admittance due to any interconnect tree at the output of a gate.

Recall that **Observation 2** gave a recursive expression for the transfer function coefficients. A similar approach can be used to derive the coefficients of both the numerator and denominator polynomial for the driving point admittance (or impedance) function. In Figure 2, the driving point admittance at node I is[8]

$$Y(s) = \frac{I_I(s)}{V_I(s)}$$

Substituting for $V_I(s)$ using the transfer function definition $H(s) = \frac{V_T(s)}{V_I(s)} = \frac{1}{B(s)}$, the admittance is given by

$$Y(s) = \frac{I_I(s)}{V_T(s)} \cdot \frac{1}{B(s)} = \frac{A(s)}{B(s)}$$

where $B(s) = (1 + b_1^I s + b_2^I s^2 + \ldots)$ is same as the denominator polynomial of the transfer function. Recall from Equations (14) - (15) that the coefficients b_K^I's are given by

$$\begin{aligned} b_1^I &= R_I(\sum_{j=1}^{N} C_j + C_T) + \sum_{j=1}^{N} C_j \sum_{i=j}^{N} R_i + C_T \sum_{i=1}^{N} R_i \\ b_k^I &= R_I \sum_{j=1}^{N} C_j b_{k-1}^j + \sum_{j=1}^{N} C_j b_{k-1}^j \sum_{i=j}^{N} R_i + L_I \sum_{j=1}^{N} C_j b_{k-2}^j + \sum_{j=1}^{N} C_j b_{k-2}^j \sum_{i=j}^{N} L_i \end{aligned}$$

The polynomial $A(s)$ is used to represent the current relative to the output voltage and is expressed as $A(s) = (a_0^I + a_1^I s + a_2^I s^2 + \ldots)$. From KCL, the current at node $N+1$ for the N segment equivalent circuit in Figure 13 is

$$\begin{aligned} I_{N+1}(s) &= sC_N V_N(s) + I_N(s) \\ &= \sum_{j=1}^{N} sC_j V_j(s) + sC_T V_T(s) \end{aligned} \tag{29}$$

where the load current is $I_T(s) = \frac{V_T(s)}{Z_T}$. Write the ratio of current to load voltage, and the ratio

[8] The driving point impedance is given by, $Z(s) = \frac{1}{Y(s)}$.

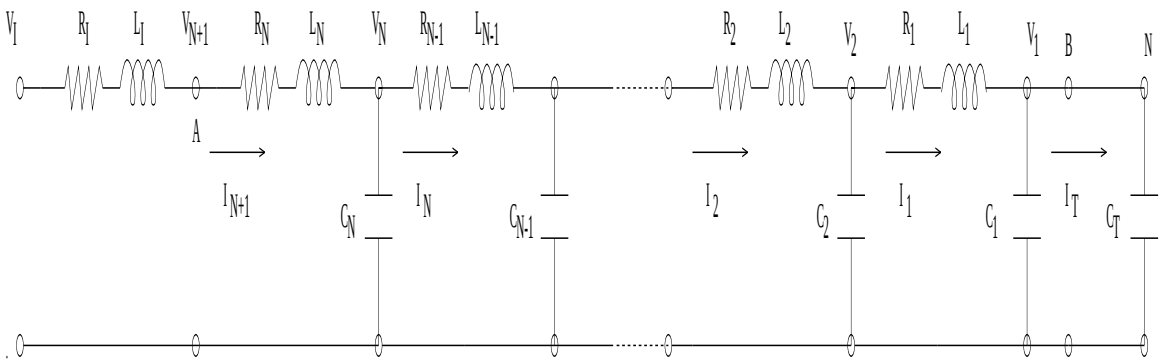

Figure 13: N-segment RLC equivalent circuit to model distributed RLC line.

of voltages, as series in s, i.e.,

$$\frac{I_j(s)}{V_T(s)} = a_0^j + a_1^j s + a_2^j s^2 + \ldots$$

and

$$\frac{V_j(s)}{V_T(s)} = 1 + b_1^j s + b_2^j s^2 + b_3^j s^3 + ...$$

Substituting in Equation (29) and collecting terms for the coefficients of s^k (for $k \geq 1$), we get[9]

$$a_k^I \quad = \quad C_N b_{k-1}^N + a_k^N = \sum_{j=1}^{N} C_j b_{k-1}^j \tag{30}$$

and for RLC lines the coefficient $a_0^j \equiv 0$. Note that a_k^I is same as a_k^{N+1} as the current through source impedance (i.e., R_I segment) is same as the current flowing through R_N segment. In general, the admittance can be expressed as an infinite series

$$Y(s) = \sum_{i=1}^{\infty} A_i s^i$$

where A_i represents the i^{th} moment of the admittance function. The moments of the driving point admittance can be expressed in terms of the coefficients a_k and b_k using the Equation (5) as

$$A_k = -\sum_{i=1}^{k} b_i A_{k-i} + a_k$$

Example: Using the above result we now compute the first few coefficients for the distributed line by considering uniform segment values with $R_j = \frac{R}{N}$, $L_j = \frac{L}{N}$ and $C_j = \frac{C}{N}$ and with number

[9]Note that a_k^{N+1} is the same as a_k^I because the currents at both nodes are equal.

of segments tending to infinity. It can be easily shown that $a_1^I = C + C_T$. The coefficient of s^2 is given by

$$\begin{aligned}
a_2^I &= \lim_{N\to\infty} \sum_{j=1}^{N} C_j b_1^j \\
&= \lim_{N\to\infty} \sum_{j=1}^{N} C_j \sum_{l=1}^{j} C_l \sum_{i=l}^{j} R_i + C_T \sum_{j=1}^{N} C_j \sum_{i=1}^{j} R_i \\
&= \lim_{N\to\infty} \frac{RC^2}{N^3} \sum_{j=1}^{N} \left(\sum_{l=1}^{j} (j-l+1) \right) + \frac{RCC_T}{N^2} \sum_{j=1}^{N} j \\
&= \lim_{N\to\infty} \frac{RC^2}{N^3} \sum_{j=1}^{N} \frac{j(j+1)}{2} + \frac{RCC_T}{N^2} \frac{N(N+1)}{2} \\
&= \lim_{N\to\infty} \frac{RC^2}{N^3} \left(\frac{N(N+1)(2N+1)}{6} + \frac{N(N+1)}{2} \right) + \frac{RCC_T}{N^2} \frac{N(N+1)}{2} \\
&= \frac{RC^2}{6} + \frac{RCC_T}{2}
\end{aligned} \tag{31}$$

Similarly, the third coefficient of the numerator polynomial for the impedance function is

$$a_3^I = \frac{R^2C^3}{120} + \frac{R^2C^2C_T}{24} + \frac{LC^2}{6} + \frac{LCC_T}{2} \tag{32}$$

An alternate way to obtain the coefficients for the driving point admittance is through the 2-port analysis. We can verify the above admittance coefficients for the RLC distributed lines by calculating directly from the 2-port parameters of Equation (8). In other words, the admittance at node I is

$$\begin{aligned}
Y(s) &= \frac{\cosh(\theta h)\frac{1}{Z_T} + \sinh(\theta h)\frac{1}{Z_0}}{\cosh(\theta h)\left(1 + \frac{Z_I}{Z_T}\right) + \sinh(\theta h)\left(\frac{Z_I}{Z_0} + \frac{Z_0}{Z_T}\right)} \\
&= \frac{a_1^I s + a_2^I s^2 + a_3^I s^3 + \ldots}{1 + b_1^I s + b_2^I s^2 + b_3^I s^3 + \ldots}
\end{aligned} \tag{33}$$

where b_1^I and b_2^I are as in Equation (10) and the coefficients a_k are given by

$$\begin{aligned}
a_1^I &= C + C_T \\
a_2^I &= \frac{RC^2}{6} + \frac{RCC_T}{2} \\
a_3^I &= \frac{R^2C^3}{120} + \frac{R^2C^2C_T}{24} + \frac{LC^2}{6} + \frac{LCC_T}{2}
\end{aligned} \tag{34}$$

Note that the coefficients a_k's are independent of the source impedance.

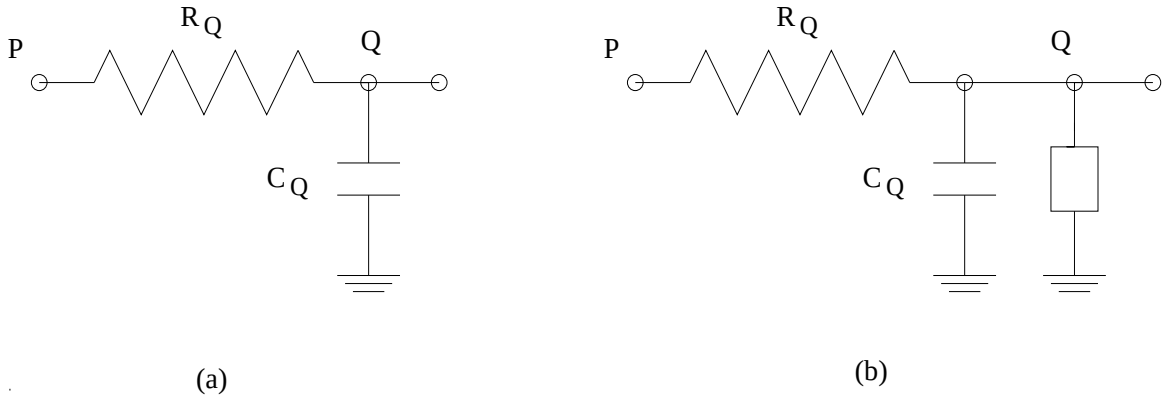

Figure 14: A single RC and RY segment in an interconnection tree.

Relationship Between Coefficients of Transfer function and Driving Point Admittance

We make a new interesting observation, and show that computing the transfer function coefficients alone is enough to calculate the driving point admittance for interconnection trees. Actually, the "Weighted Capacitance" term ($WC(N,k) = \sum_{j=1}^{N} C_j b_{k-1}^{j}$) in the transfer function coefficient b_k in Equation (14) is same as the input impedance denominator polynomial coefficient in Equation (30). In general for RLY trees the "Weighted Admittance" term ($WY(N,k) = \sum_{l=1}^{k} Y_{l,N} b_{k-l}^{N}$) is same as the driving point admittance numerator polynomial coefficients (a_k). Therefore, during the b_k coefficient computation, if we compute weighted capacitance (or admittance) term and store it separately then the driving point admittance can be directly calculated, which results in good time saving.

Algorithm 5: Admittance_coefficients(N,k)
Input: Coefficients $a(N,l)$ and $b(N,l)$ for $l = 1,\ldots k$
Output: $Y_{l,N}$ for $l = 1,\ldots k$
for $l = 1,\ldots k$ $Y_{l,N} = -\sum_{i=1}^{k} b_i Y_{k-i,N} + a_l$ return

In [26] Sriram and Kang proposed a two step procedure for computing the transfer function at any node of an interconnection tree. The first involves computing the admittance at each node of the tree and the second step is to compute the transfer function coefficients using the admittance at each node as a series expansion. But from the above observation that a_k term is same as

Algorithm 6: Single_Pass_Transfer_Coefficient$(I, N1, N2, k)$

Input: Interconnection Tree $T(I)$; Source node I,
Target node $N1$ with $N2$ as son ($N2 = 0$ for leaf node),
and Required Moment Order k

Output: Transfer function Coefficient $b(I, k)$

```
if N1 is a leaf node (or if N2 = 0)
  if k ≥ 3 then b(N1,k) = 0, a(N1,k) = 0, and d(N1,k) = 0
  if k = 2 then b(N1,k) = 0, a(N1,k) = 0, and d(N1,k) = C_N1
  if k = 1 then b(N1,k) = 0, a(N1,k) = C_N1, and d(N1,k) = 0
  if k = 0 then b(N1,k) = 1, a(N1,k) = 0, and d(N1,k) = 0
  Compute Admittance_coefficients(N1,k)
  (i.e for l = 1,...k Y_{k,N1}
else
  a(N1,k) = a(N2,k) + Σ_{l=1}^{k} Y_{l,N1} b^N_{k-l}
  d(N1,k) = d(N2,k) + Σ_{l=1}^{k} Y_{l,N1} b^N_{k-1-l}
  b(N1,k) = b(N2,k) + R_N a(N2,k) + L_N d(N2,k)
  Compute Admittance_coefficients(N1,k)
  (i.e for l = 1,...k Y_(k,N1

for each node j ∈ S(N1) and j ≠ N2
  if j is a leaf node
    Single_Pass_Transfer_Coefficient(I,j,0,k)
  else
    for each node m ∈ S(j)
      Single_Pass_Transfer_Coefficient(I,j,m,k)
  Add all Admittance coefficients (i.e., Y_{l,j} for l = 1,
  ...k) at each node with mutiple childs.

return
```

weighted admittance, we can compute admittance polynomial at each node recursively and in the same calculation we can also obtain the transfer function coefficients. Therefore, by careful recursive computation of b_k and keep aside the term corresponding to a_k we can reduce the two step procedure to just one "single pass" analysis of the interconnection tree. We present the "Single_Pass_Transfer_Coefficient" algorithm which combines the two step procedure of [26, 27]. In Algorithm 5, we used d_k to represent the weighted admittance corresponding to inductance term. Even though the time complexity is still going to be linear in number of nets in the tree, in practice computation time is almost reduced by half.

Example: We illustrate the relationship between weighted capacitance (or admittance) by con-

sidering one segment of an RLC equivalent circuit as shown in Figure 14. The k^{th} transfer function coefficient at the node P can be obtained using recursive expression in **Observation 2** as

$$b_k^P = R_Q \sum_{i \in Subtree(Q)} C_i b_{k-1}^i + b_K^Q$$

and the driving point admittance coefficient is

$$a_k^P = \sum_{i \in Subtree(Q)} C_i b_{k-1}^i$$

Therefore, the driving point admittance at the node P is given by

$$Y(s)^P = \frac{\sum_{k=1}^{\infty} a_k^P s^k}{\sum_{k=0}^{\infty} b_k^P s^k}$$

We extend this analysis for a general RLY interconnection tree by considering again one segment as shown in Figure 14b. The k^{th} transfer function and admittance coefficients at the node P are:

$$b_k^P = R_Q \sum_{l=1}^{k} \sum_{i \in Subtree(Q)} Y_{l,j} b_{k-l}^i + b_K^Q$$

$$a_k^P = \sum_{l=1}^{k} \sum_{i \in Subtree(Q)} Y_{l,j} b_{k-l}^i$$

where $Y_Q(s) = sY_{1,Q} + s^2 Y_{2,Q} + \ldots$.

7 Experimental Results

We now give a practical demonstration of the utility of our non-uniform equivalent circuit models, in the context of the two-pole simulation methodology. We study the same interconnect tree analyzed in [34] (see Figure 6) over a wide range of interconnect parameters [30], driver resistance, load capacitance, and grid size. For the tree analysis we use the "standard two-pole method" (described in the Appendix A) and calculate the first and second moments of the transfer function of the main path. In computing the moments of the tree, we represent the off-path subtrees by their respective admittance values instead of approximating by total subtree capacitance. We have tried replacing each interconnect line of the tree by both of the general non-uniform segment models given in Equation (20) and Equation (21). Since both models gave very similar responses, the following data refer to the three non-uniform **L** segment model (Equation (20)) only.

We compared our results with several other methods:

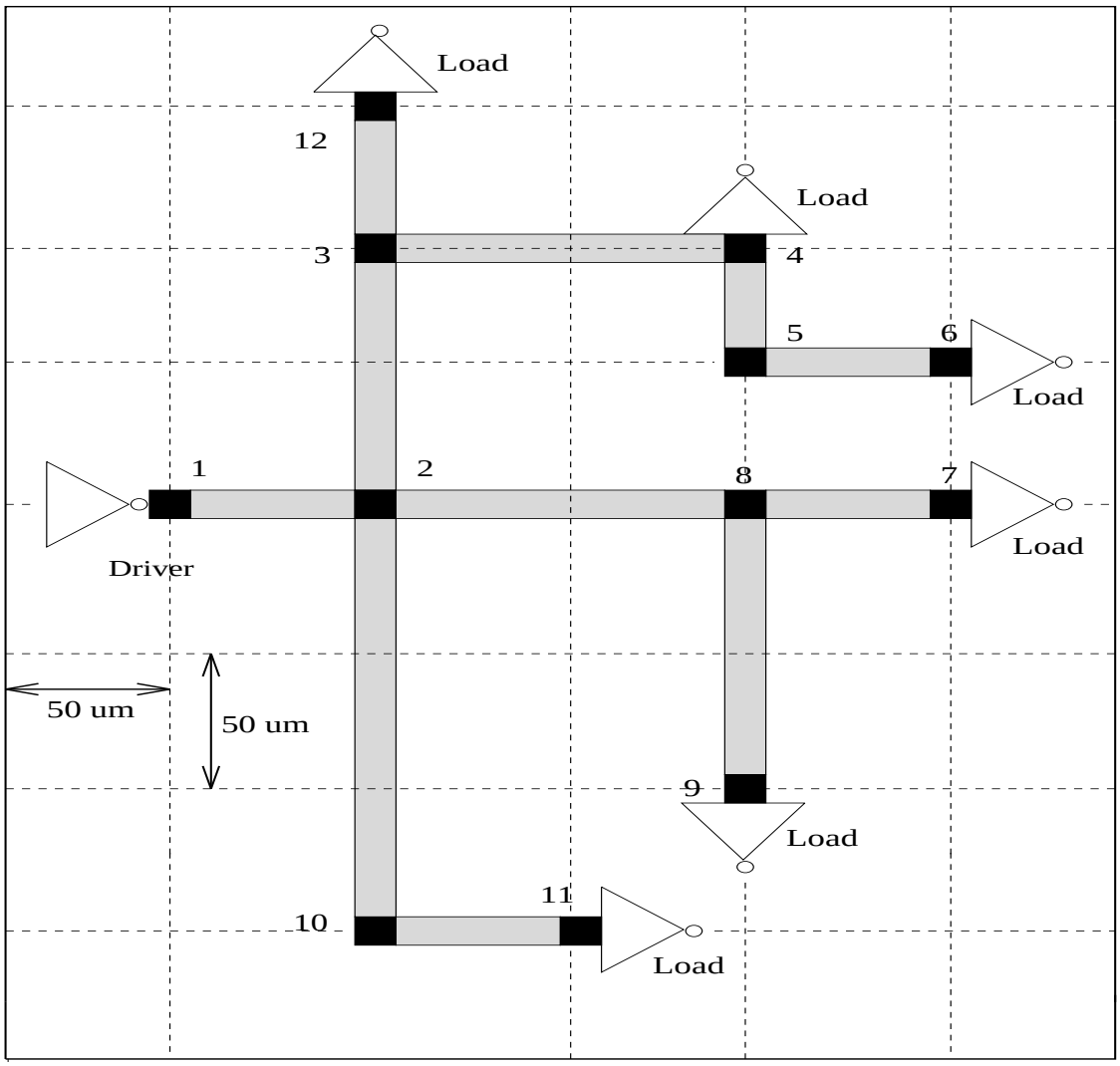

Figure 15: A tree interconnection layout studied in [ZSTGC94], shown with grid size = $50\mu m$.

- The SPICE **LTRA** (Lossy TRAnsmission line)[10] model which represents each interconnect line in the tree as a lossy transmission line. The LTRA model calculates the response using the convolution of the transmission line's impulse response with the input response [21].
- We also calculated response and delay using the method of Zhou et al. [34] with each interconnect line represented by three uniform **L** segments.
- Finally, we also used the single dominant pole method [9] and calculated delays using the widely used Elmore delay model.

[10]This model is also referred to as a uniform transmission line model because it has constant resistance, capacitance and inductance per unit length.

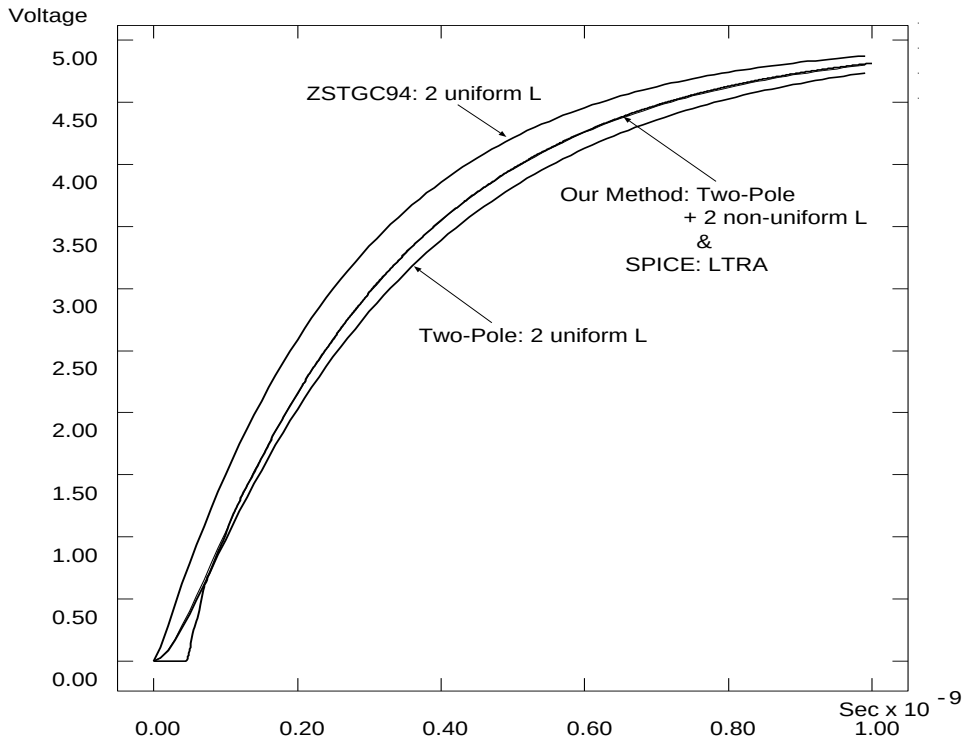

Figure 16: Step response at Node 6 for the tree topology in Figure 13. We compare the uniform/non-uniform models using the Stan2Pole method against SPICE simulations and the method of [ZSTGC94].

A simple comparison of these various methods is shown in Figure 16, which plots the voltage response at Node 6 with a driver resistance of 150Ω, a load capacitance of 2 pf, interconnect parameters $R = 0.015\ \Omega$, $C = 0.176\ fF$, $L = 0.246\ pH$ per μm interconnect length, and a grid size of 500 μm. For this comparison only, we used two-segment uniform and non-uniform models. The response calculated using our non-uniform model is very similar to the SPICE LTRA simulation. In a more detailed comparison, we have calculated the voltage response at a specific node (Node 6) using each of the four distinct simulation methodologies, and determined the 90% threshold delay for wide range of interconnect parameters[11]. The delay values using the different methods are given for typical VLSI interconnects in Table 2 and for typical MCM parameters [30] in Table 3. We see that as wire length increases, the difference between these models becomes much more significant. The time taken for SPICE simulation varies from few minutes to few hours, whereas the two-pole simulation takes at most a few seconds. Specifically, the simulation

[11] Here, the delay refers to the total delay including the propagation delay. In Appendix D we discussed the method to compute only the rise-time delay.

Driver res. Ω	**Load cap.** pF	**Grid size** μm	**SPICE LTRA Delay**(ps)	**Two-pole with New Model Delay**(ps)	**[ZSTGC94] Two-pole Delay**(ps)	**Elmore (single-pole) Delay**(ps)
10	0.002	50	4	**4**	4	4
100	0.002	50	36	**37**	30	38
1000	0.002	50	372	**373**	303	372
10	0.2	50	28	**30**	25	38
100	0.2	50	317	**316**	258	318
1000	0.2	50	3085	**3114**	2532	3111
10	2.0	50	330	**325**	275	342
100	2.0	50	2854	**2846**	2325	2860
10	2.0	500	861	**857**	789	987
10	2.0	50	379	**399**	347	342
10	20.0	50	3284	**3249**	2752	3385

Table 2: The 90% threshold delay values at Node 6 using SPICE LTRA, two-pole and single-pole methodologies. The interconnect parameters are $R = 0.015\ \Omega/\mu m$, $C = 0.176\ fF/\mu m$, and $L = 0.246\ pH/\mu m$.

speedup obtained using new models within the two-pole methodology is between 2 to 3 orders of magnitude compared to SPICE. For high-speed systems, or for MCM layout applications where the wire lengths become very large, our approach clearly allows improved accuracy and efficiency when compared with previous two-pole methods.

8 Conclusions

For high-speed systems, accurate estimation of the propagation delays due to interconnects is one of the main obstacles for correct system implementation. In this paper, we simulated interconnect

Interconnect parameters /μm	**Driver res.** Ω	**Load cap.** pF	**Grid size** μm	**SPICE LTRA Delay**(ps)	**Two-pole with New Model Delay**(ps)	**ZSTGC94 Two-pole Delay**(ps)	**Elmore Delay)** ps
$R = 0.0015\ \Omega$ $C = 0.176\ fF$ $L = 0.246\ pH$	10	2.0	50	298	**284**	228	283
$R = 0.0015\ \Omega$ $C = 0.176\ fF$ $L = 0.246\ pH$	10	2.0	500	299	**321**	266	380
$R = 0.0015\ \Omega$ $C = 0.176\ fF$ $L = 0.246\ pH$	10	2.0	5000	1424	**1469**	1306	1795
$R = 0.015\ \Omega$ $C = 0.176\ fF$ $L = 24.6\ pH$	10	2.0	50	379	**399**	347	342
$R = 0.015\ \Omega$ $C = 17.6\ fF$ $L = 0.246\ pH$	10	2.0	50	707	**708**	507	738
$R = 0.15\ \Omega$ $C = 0.176\ fF$ $L = 0.246\ pH$	10	2.0	50	751	**800**	736	906
$R = 0.015\ \Omega$ $C = 0.176\ fF$ $L = 0.246\ pH$	10	20.0	50	3284	**3249**	2752	3385

Table 3: The 90% threshold delay values for a wide range of MCM parameters at Node 6 using SPICE LTRA, two-pole and single-pole methodologies.

trees by modeling each interconnect line using new non-uniform lumped segment models and the two-pole methodology. We have also given a general recursive expression for computing the coefficient b_k of the transfer function of the interconnect tree. (Although we use the two-pole method to demonstrate the advantage of new models, the approach can be extended to derive a k^{th} order moment matching model and calculate the k-pole response.) For a wide range of VLSI and MCM interconnect parameters the delay estimates using the new models are within 8% of SPICE-computed delays. The simulation speed attained using new models is 3 orders of magnitude faster than SPICE, and our approach is also more efficient and accurate than previous methods which employed a large number of uniform RLC segments. (Possibly, evaluations of existing routing tree techniques (such as Elmore routing trees [1] or A-trees [2]), whose delays

were measured using the technique of [34], may change.) Finally, our non-uniform equivalent circuits can also be employed in place of the lumped **T** and **Π** models that are traditionally used for clock skew minimization and other performance-driven routing applications. We believe that these advantages will be significant for critical timing analyses in the design of high-speed integrated circuits and multichip module designs. In the future, we would like to extend our methodology for more general topologies such as mesh networks.

We also make a new interesting observation, and show that computing the transfer function coefficients alone is enough to calculate the driving point admittance for interconnection trees. With this technique the two phase transfer function coefficient computation for interconnection trees in [26] can be reduced to "single phase" and reducing critical time complexity. We also present a new "open-ended **Π** model", to better capture the gate delay and output rise time for current interconnect trees.

References

[1] K. D. Boese, A. B. Kahng and G. Robins, "High-Performance Routing Trees With Identified Critical Sinks", *Proc. 30th ACM/IEEE Design Automation Conf.*, June 1993, pp. 182-187.

[2] J. Cong, K. S. Leung and D. Zhou, "Performance-Driven Interconnect Design Based on Distributed RC Delay Model", *Proc. 30th ACM/IEEE Design Automation Conf.*, June 1993, pp. 606-611.

[3] A. Deustch et al., "High-speed Signal Propagation on Lossy Transmission Lines", *IBM Journal Research and Development*, July 1990, pp. 601-615.

[4] W. C. Elmore, "The Transient Response of Damped Linear Networks with Particular Regard to Wideband Amplifiers", *Journal of Applied Physics* 19, Jan. 1948, pp. 55-63.

[5] L. Gerzberg, "Monolithic Power-Spectrum Centroid Detector", *PhD Thesis*, Stanford University, May 1979.

[6] M. S. Ghausi and J. J. Kelly, *Introduction to Distributed-Parameter Networks: With Application to Integrated Circuits*, New York: Holt, Rinehart and Winston, 1968.

[7] N. Gopal, Dean P. Neikirk and L. T. Pillage, "Evaluating RC-Interconnect Using Moment-Matching Approximations", *Proc. IEEE International Conference on Computer-Aided Design*, June 1991, pp. 74-77.

[8] D. S. Gao, D. Zhou, "Propagation Delay in RLC Interconnection Networks", *Int. Symposium on Circuits and Systems*, May 1993, pp. 2125-2128.

[9] M. A. Horowitz, "Timing Models for MOS Circuits", *PhD Thesis*, Stanford University, Jan. 1984.

[10] A. B. Kahng and S. Muddu "Delay Estimation of Trees using Two-pole method and Optimal Equivalent Circuits", *UCLA CS Dept. TR-930035*, October 1993.

[11] A. B. Kahng and S. Muddu, "A General Methodology for Response and Delay Computations in VLSI Interconnects", *UCLA CS Dept. TR-940015*, March 1994, extended version submitted to IEEE Trans. on CAD.

[12] A. B. Kahng and S. Muddu, "Optimal Equivalent Circuits for Interconnect Delay Calculations Using Moments", *Proc. ACM/IEEE European Design Automation Conf.*, September 1994, pp. 164-169.

[13] A. B. Kahng and S. Muddu, "Two-pole Analysis of Interconnection Trees", *Proc. IEEE MCMC Conf.*, January 1995, pp. 105-110.

[LK92] S. Lin and E. S. Kuh, " Transient Simulation of Lossy Interconnects Based on The Recursive Convolution Formulation", *IEEE Trans. Circuits and Systems*, Nov. 1992, pp. 869-878.

[14] P. R. O'Brien and T. L. Savarino, "Modeling the Driving-Point Characteristic of Resistive Interconnect for Accurate Delay Estimation", *Proc. IEEE ICCAD*, 1989, pp. 512-515.

[15] P. R. O'Brien and T. L. Savarino, "Efficient On-Chip Delay Estimation for Leaky Models of Multiple-Source Net", *IEEE Custom Integrated Circuits Conf.*, 1990.

[16] U. Kumar, "Modeling of Distributed Lossless and Lossy Structures: A Review", *IEEE Circuits and Systems Magazine* 2(3), 1980, pp. 12-16.

[17] S. P. McCormick, "Modeling and Simulation of VLSI Interconnections with Moments", *PhD Thesis*, MIT, June 1989.

[18] L. T. Pillage and R. A. Rohrer, "Asymptotic Waveform Evaluation for Timing Analysis", *IEEE Trans. CAD*, Apr. 1990, pp. 352-366.

IEEE Trans. on CAD, December 1994, pp. 1526-1535.

[19] Y. V. Rajput, "Modelling Distributed *RC* Lines for the Transient Analysis of Complex Networks", *Int. Journal of Electronics* 36(5), 1974, pp. 709-717.

[20] C. L. Ratzlaff and L. T. Pillage, "RICE: Rapid Interconnect Circuit Evaluation Using AWE", *IEEE Tras. CAD*, June 1994, pp. 764-776.

[21] J. S. Roychowdhury and D. O. Pederson, "Efficient Transient Simulation of Lossy Interconnect", *Proc. 28th ACM/IEEE Design Automation Conf.*, June 1991, pp. 740-745.

[22] J. Rubinstein, P. Penfield and M. A. Horowitz, "Signal Delay in RC Tree Networks", *IEEE Trans. on CAD* 2(3), July 1983, pp. 202-211.

[23] C. Ratzlaff, S. Pullela, and L. Pillage, "Modeling the *RC* interconnect effects in a hierarchical timing analyzer", *Proc. Custom Integrated Circuits Conference*, May 1992.

[24] T. Sakurai, "Approximation of Wiring Delay in MOSFET LSI", *IEEE Journal of Solid-State Circuits*, Aug. 1983, Vol.18, No.4, pp. 418-426.

[25] M. Sriram and S. M. Kang, "Performance driven MCM Routing Using a Second Order RLC Tree Delay Model", *Proc. IEEE Intl. Conf. on Wafer Scale Integration*, Jan. 1993, pp. 262-267.

[26] M. Sriram and S. M. Kang, "Fast Approximation of The Transient Response of Lossy Transmission Line Trees", *Proc. 30th ACM/IEEE Design Automation Conf.*, June 1993, pp. 691-696.

[27] M. Sriram and S. M. Kang, "Physical Design for Multichip Modules", Kluwer Academic Publishers, 1994.

[28] T. Tang, M. Nakhla, and R. Griffith, "Analysis of Lossy Multiconductor Transmission Lines Using The Asymptotic Waveform Evaluation Technique", *IEEE Trans. Microwave Theory and Techniques*, Dec. 1991, pp. 2107-2116.

[29] Synposys, "Design Compiler Family Reference Manual", version 3.3a, March 1995.

[30] D. B. Tuckerman, *Personal communication*, Jan. 1995.

[31] J. White, L. Pillage, and J. Cohn, "Computer-Aided Analysis and Design of Interconnect", *ICCAD Tutorial 2*, Nov. 1993, pp. 24-26.

[32] Q. Yu and E. S. Kuh, "Exact Moment Matching Model of Transmission Lines and Application to Interconnect Delay Estimation", *IEEE Trans. VLSI Systems*, 1995, pp. 311-322.

[33] D. Zhou, F. P. Preparata and S. M. Kang, "Interconnection Delay in Very High-Speed VLSI", *IEEE Trans. on Circuits and Systems* 38(7), July 1991, pp. 779-790.

[34] D. Zhou, S. Su, F. Tsui, D. S. Gao and J. S. Cong, "A Simplified Synthesis of Transmission Lines with A Tree Structure", *Intl. Journal of Analog Integrated Circuits and Signal Processing*, Jan. 1994, pp. 19-30.

[35] D. Zhou, F. Tsui and D. S. Gao, "High Performance Multichip Interconnection Design", *Proceedings of the 4th ACM/SIGDA VLSI Physical Design Workshop*, April 1993, pp. 32-43.

Appendix A: Standard Two-pole Methodology

The transfer function of the system considering two dominant poles is

$$H(s) = \frac{k_1}{s - s_1} + \frac{k_2}{s - s_2}$$

where s_1, s_2 are the poles and k_1, k_2 are the coefficients corresponding to the poles. Assuming a step input, $V_{in}(t) = V_0 u(t)$, $V_{in}(s) = \frac{V_0}{s}$, and the output voltage is, $V_{out}(s) = V_0 \frac{H(s)}{s}$. Applying partial fractions and taking the inverse Laplace transform:

$$v_{out}(t) = \left(-(\frac{k_1}{s_1} + \frac{k_2}{s_2}) + \frac{k_1}{s_1} e^{s_1 t} + \frac{k_2}{s_2} e^{s_2 t} \right)$$

Then using the boundary conditions $v_{out}(t \to \infty) = V_0$ and $v'_{out}(t = 0) = 0$, one can solve for s_1, s_2, k_1, k_2. Therefore,

$$-(\frac{k_1}{s_1} + \frac{k_2}{s_2}) = 1; k_1 + k_2 = 0$$

and the time-domain response is

$$v_{out}(t) = \left(1 + \frac{k_1}{s_1} e^{s_1 t} + \frac{k_2}{s_2} e^{s_2 t} \right)$$

Now by applying the definition of moments to the two-pole transfer function, we get

$$(\frac{k_1}{s_1^2} + \frac{k_2}{s_2^2}) = M_1; \quad (\frac{k_1}{s_1^3} + \frac{k_2}{s_2^3}) = M_2$$

and solving the above equations yields

$$s_{1,2} = \frac{2}{-M_1 \pm \sqrt{4M_2 - 3M_1^2}}; \quad k_1 = -k_2 = -\frac{1}{\sqrt{4M_2 - 3M_1^2}}$$

Note that the poles of the system should be always in the left half of the $s-$plane for stable systems. The voltage response can be calculated for both real and complex poles as follows:

Case 1: Real Poles.

From the above equations,

$$k_1 = -\frac{s_1 s_2}{s_2 - s_1}; \quad k_2 = \frac{s_1 s_2}{s_2 - s_1}$$

The voltage response for real poles is

$$v_{out}(t) = V_0 (1 - \frac{s_2}{s_2 - s_1} e^{s_1 t} - \frac{s_1}{s_1 - s_2} e^{s_2 t}) \tag{35}$$

Case 2: Complex Poles.

Since the poles are complex we can express them in the form $s_1 = -\alpha + \jmath\beta$ and $s_2 = -\alpha - \jmath\beta$.

The voltage response is

$$\begin{aligned} v_{out}(t) &= V_0\left[1 - \frac{s_2}{s_2 - s_1}e^{s_1 t} - \frac{s_1}{s_1 - s_2}e^{s_2 t}\right] = V_0\left[1 - \frac{e^{-\alpha t}}{2}\left((1 + \frac{\alpha}{\jmath\beta})e^{\jmath\beta t} + (1 - \frac{\alpha}{\jmath\beta})e^{-\jmath\beta t}\right)\right] \\ &= V_0\left[1 - e^{-\alpha t}(\cos(\beta t) + \frac{\alpha}{\beta}\sin(\beta t))\right] = V_0\left[1 - \frac{\sqrt{\alpha^2 + \beta^2}}{\beta}e^{-\alpha t}\sin(\beta t + \rho)\right] \end{aligned}$$

where $\rho = \tan^{-1}(\frac{\beta}{\alpha})$ and

$$\alpha = \frac{M_1}{2(M_1^2 - M_2)}; \quad \beta = \frac{\sqrt{3M_1^2 - 4M_2}}{2(M_1^2 - M_2)}$$

Appendix B: Non-Uniform Segment Computation for General Interconnect with Load and Source Impedances

Consider non-uniform equivalent circuits to match first and second coefficients, b_1^S and b_2^S. The system of nonlinear of equations for 3 non-uniform L segments are:

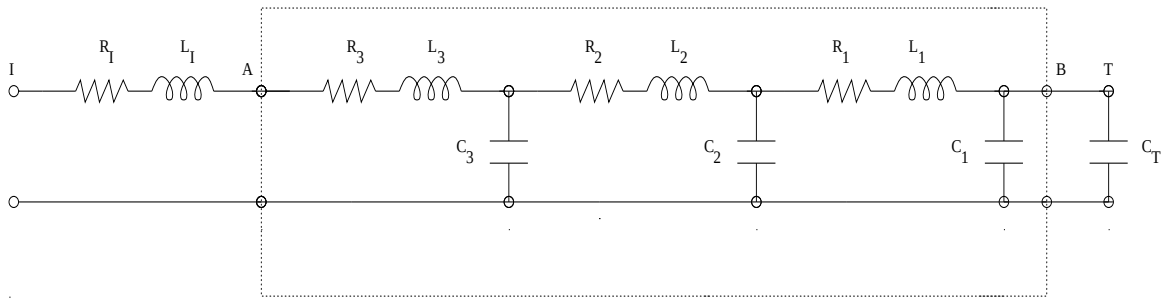

Figure 17: Three L segment model.

$$
\begin{aligned}
R_1 + R_2 + R_3 &= R \\
C_1 + C_2 + C_3 &= C \\
R_3(C_1 + C_2 + C_3) + R_2(C_2 + C_3) + R_1C_1 &= \frac{RC}{2} \\
R_2R_3C_2C_3 + R_1R_3C_1C_3 + R_1R_2C_1C_2 + R_1R_3C_2C_1 + R_2R_3C_1C_3 &= \frac{(RC)^2}{24} \\
R_2C_3(C_1 + C_2) + R_1C_1C_3 + R_1C_2C_1 &= \frac{RC^2}{6} \\
C_3(R_1 + R_2) + R_1C_2 &= \frac{RC}{2} \\
R_1R_3C_3 + R_1R_2C_2 + R_1R_3C_2 + R_2R_3C_3 &= \frac{R^2C}{6} \qquad (36)
\end{aligned}
$$

The optimized circuit elements are

$$R_1 = 0.40R, \qquad R_2 = 0.40R, \qquad R_3 = 0.20R$$

$$C_1 = 0.17C, \qquad C_2 = 0.41C, \qquad C_3 = 0.42C$$

For RLC segments Figure 17 the inductance values are in the same ratio as for resistance values, i.e.,

$$L_1 = 0.40L, \qquad L_2 = 0.40L, \qquad L_3 = 0.20L$$

which imply the following coefficients in the transfer function:

$$b_1^{IB} = R_IC + R_IC_T + \frac{RC}{2} + RC_T$$

$$b_2^{IB} = \frac{R_I R C^2}{6.49} + \frac{R_I R C C_T}{2} + \frac{(RC)^2}{23.85} + \frac{R^2 C C_T}{6.13} + L_I C + L_I C_T + \frac{LC}{2} + L C_T$$

Similarly the system of equations for 3 non-uniform Π segments are:

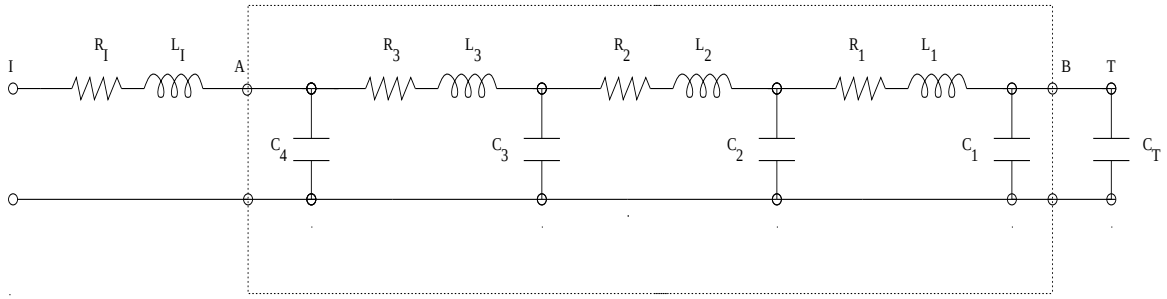

Figure 18: Three Π segment model.

$$\begin{aligned}
R_1 + R_2 + R_3 &= R \\
C_1 + C_2 + C_3 + C_4 &= C \\
R_3(C_1 + C_2 + C_3) + R_2(C_2 + C_1) + R_1 C_1 &= \frac{RC}{2} \\
R_2 R_3 C_2 C_3 + R_1 R_3 C_1 C_3 + R_1 R_2 C_1 C_2 + R_1 R_3 C_2 C_1 + R_2 R_3 C_1 C_3 &= \frac{(RC)^2}{24} \\
R_3 C_4(C_1 + C_2 + C_3) + R_2 C_4(C_1 + C_2) + R_1 C_1 C_4 + R_2 C_3(C_1 + C_2) + R_1 C_1 C_3 + R_1 C_2 C_1 &= \frac{RC^2}{6} \\
C_4(R_1 + R_2 + R_3) + C_3(R_1 + R_2) + R_1 C_2 &= \frac{RC}{2} \\
R_1 R_3 C_3 + R_1 R_2 C_2 + R_1 R_3 C_2 + R_2 R_3 C_3 &= \frac{R^2 C}{6}
\end{aligned} \tag{37}$$

The optimized circuit elements are

$$R_1 = 0.34R, \qquad R_2 = 0.32R, \qquad R_3 = 0.34R$$

$$C_1 = 0.15C, \qquad C_2 = 0.35C, \qquad C_3 = 0.35C \qquad C_0 = 0.15C$$

Taking inductance values in the same ratio as resistance values yields

$$L_1 = 0.34L, \qquad L_2 = 0.32L, \qquad L_3 = 0.34L$$

implying

$$\begin{aligned}
b_1^{IB} &= R_I C + R_I C_T + \frac{RC}{2} + R C_T \\
b_2^{IB} &= \frac{R_I R C^2}{6.0} + \frac{R_I R C C_T}{2} + \frac{(RC)^2}{27.11} + \frac{R^2 C C_T}{6.37} + L_I C + L_I C_T + \frac{LC}{2} + L C_T
\end{aligned}$$

Appendix C: Non-Uniform Segment Computation for Open-Ended Interconnect Lines

In this Appendix we obtain the parameters for three segment **L** and **Π** models in terms of the distributed RC line parameters. As we have pointed out in the discussion before, with **L** segment models we have an overspecified system of equations and hence in deriving the parameters we try to minimize the error in the moments of the transfer function.

L Segment Model

The open-ended transfer function for distributed RC line is obtained by substituting $L = 0$ in Equation (11),

$$H(s) = \frac{1}{1 + \frac{RC}{2}s + \frac{(RC)^2}{24}s^2 + \frac{(RC)^3}{720}s^3 + ...}$$

The open-ended transfer function for three uniform **L**-type RC segments (Figure 19) is given by

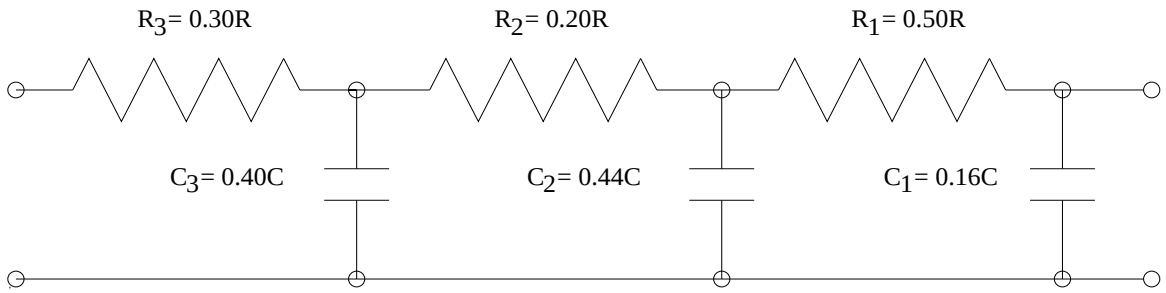

Figure 19: Non-uniform three **L** segment model for an open-ended distributed RC line.

$$H_{eq}(s) = \frac{1}{1 + b_1 s + b_2 s^2 + b_3 s^3}$$

Since the three segment RC model should match the distributed RC line transfer function up to the third moment, comparing the coefficients of s, s^2, s^3, we obtain the following equations

$$\begin{aligned} b_1 = R_3(C_1 + C_2 + C_3) + R_2(C_1 + C_2) + R_1C_1 &= \frac{RC}{2} \\ b_2 = R_2R_3C_2C_3 + R_1R_3C_1C_3 + R_1R_2C_1C_2 + R_1R_3C_2C_1 + R_2R_3C_1C_3 &= \frac{(RC)^2}{24} \\ b_3 = R_1R_2R_3C_1C_2C_3 &= \frac{(RC)^3}{720} \end{aligned} \quad (38)$$

Clearly there is no unique solution if we try to solve for the six variable parameters of the model given in (Figure 19) using the above three equations. Using the approach given in [19] we can obtain more information by calculating the open-circuit input impedance for both the

distributed RC line and for the three segment model. The open-circuit input impedance, z_{11} of the distributed RC line is given by [6]

$$z_{11} = \frac{1 + \frac{RC}{2!}s + \frac{(RC)^2}{4!}s^2 + \frac{(RC)^3}{6!} + \ldots}{\frac{C}{1!}s + \frac{RC^2}{3!}s^2 + \frac{R^2C^3}{5!}s^3 + \ldots}$$

The open-circuit input impedance for three uniform **L**-type RC segments is

$$(z_{11})_{eq} = \frac{1 + b_1 s + b_2 s^2 + b_3 s^3}{a_1 s + a_2 s^2 a_3 s^3}$$

Since the numerator polynomial of the input impedance is exactly same as the denominator polynomial of the open-ended transfer function, matching those coefficients will give same set of equations. By matching the coefficients of the denominator polynomial of input impedance, we get

$$\begin{aligned} a_1 = C_1 + C_2 + C_3 &= C \\ a_2 = R_2C_2C_3 + R_1C_1C_3 + R_2C_1C_3 + R_1C_2C_1 &= \frac{RC^2}{6} \\ a_3 = R_1R_2C_1C_2C_3 &= \frac{R^2C^3}{120} \end{aligned} \tag{39}$$

Since the sum of all the resistances should be equal to the total line resistance,

$$R_1 + R_2 + R_3 = R \tag{40}$$

The constraints derived above by matching the driving point impedance (or admittance) can also be derived by matching the transfer function coefficients of the model. To do this we need to consider the equivalent circuit with source impedance (R_I) and match the coefficients corresponding to the term R_I. This can be easily verified by examining the R_I term $(\sum_{j=1}^{N} C_j b_{k-1}^j)$ in general expression for the transfer function coefficient b_k in Equation (14) and noticing that it is same as the input impedance denominator polynomial coefficient in Equation (30).

Clearly we can not solve for the six unknown parameters $R_1, R_2, R_3, C_1, C_2, C_3$ using these seven overspecified equations. Thus, we have obtained values for these parameters by using numerical techniques to minimize the squared error in the coefficients b_1, b_2, b_3 and the model parameters are

$$R_1 = 0.50R, \qquad R_2 = 0.20R, \qquad R_3 = 0.30R$$

$$C_1 = 0.16C, \qquad C_2 = 0.44C, \qquad C_3 = 0.40C$$

Extending the model for RLC lines by using the identical distribution of inductance and resistance values, we get

$$L_1 = 0.50L, \qquad L_2 = 0.20L, \qquad L_3 = 0.30L$$

Π Segment Model

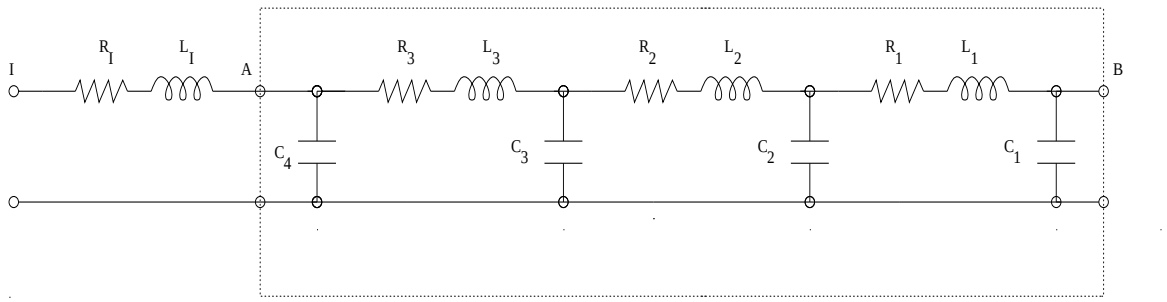

Figure 20: Non-uniform three Π segment model for an open-ended distributed RLC line.

We now extend the above technique to calculate the parameters for the Π segment equivalent circuit (Figure 20) for modeling open-ended line. The system of constraints for the Π model can be obtained by matching the transfer function coefficients corresponding to both the interconnect RC term and source R_I term. The constraints derived by comparing the pure RC term are

$$\begin{aligned}
C_1 + C_2 + C_3 + C_4 &= C \\
R_3(C_1 + C_2 + C_3) + R_2(C_1 + C_2) + R_1C_1 &= \frac{RC}{2} \\
R_2R_3C_2C_3 + R_1R_3C_1C_3 + R_1R_2C_1C_2 + R_1R_3C_2C_1 + R_2R_3C_1C_3 &= \frac{(RC)^2}{24} \\
R_1R_2R_3C_1C_2C_3 &= \frac{(RC)^3}{720}
\end{aligned} \qquad (41)$$

and the constraints corresponding to the source term R_I are

$$\begin{aligned}
R_3C_4(C_1 + C_2 + C_3) + R_2C_4(C_1 + C_2) + R_1C_1C_4 + R_2C_3(C_1 + C_2) + R_1C_1C_3 + R_1C_1C_2 &= \frac{RC^2}{6} \\
C_4(R_2R_3C_2C_3 + R_1R_3C_1C_3 + R_1R_2C_1C_2 + R_1R_3C_2C_1 + R_2R_3C_1C_3) + C3(R1R2C2C3) &= \frac{R^2C^3}{120}
\end{aligned} \qquad (42)$$

Since the sum of all the resistances should be equal to the total line resistance, we have one more constraint

$$R_1 + R_2 + R_3 = R \qquad (43)$$

Unlike the above **L** segment model, here we can solve exactly for the 7 variables using the above constraints. However, we used numerical techniques in calculating these parameters by minimize the error in the corresponding moments and the model parameters are:

$$R_1 = 0.50R, \qquad R_2 = 0.20R, \qquad R_3 = 0.30R$$

$$C_1 = 0.23C \qquad C_2 = 0.36C, \qquad C_3 = 0.30C \qquad C_0 = 0.11$$

Extending the model for RLC lines, we get

$$L_1 = 0.50L, \qquad L_2 = 0.20L, \qquad L_3 = 0.30L$$

For open-ended line models both our method and Yu and Kuh's method [32] are similar and the constraints generating are also identical. Their two segment open-ended model match our model given in [12]. But their optimization method (MATLAB) used to derive the model parameters is different from our method, and hence for three segment models we have slightly different parameter values. We note that our models yield less squared error in the moments of the transfer function compared to the model presented in [32].

Appendix D: Rise-time Delay vs Total Delay for Interconnect Trees

Propagation delay (or time-of-flight) T_{pd} in any transmission line is defined as the finite time it takes for an electromagnetic signal to travel from one point to the other in a transmission line. For an interconnect line of length h and inductance l, capacitance c per unit length, the propagation delay is

$$T_{pd} = h\sqrt{lc}$$

Because of the finite propagation delay, the response at the output will be zero until T_{pd} and then it follows the input. In our interconnect trees analysis, since we computed the two-pole response at any sink node by modeling the lines using the distributed transmission line models, the voltage response includes the time taken for the signal to propagate from source to the sink. But the two-pole response, which consists of exponential functions, starts rising from $t = 0$, even though the actual response has no signal between $0 \leq t \leq T_{pd}$. The delay computed from the two-pole response includes both propagation and rise time delay. The original transfer function is

$$\frac{v_{out}}{v_{in}} = \frac{1}{\sum_{i=0}^{n} b_i s^i}$$

To eliminate any possible errors due to the the behavior of signal during $0 \leq t \leq T_{pd}$, we modify the transfer function such that the propagation delay term can be extracted out. Basically, we will compute new transfer function ($\frac{v'_{out}}{v_{in}}$) coefficients and poles without considering the propagation delay inherently. The final time-domain response can be computed back by time-shifting the signal to the right by T_{pd}.

$$\frac{v'_{out}}{v_{in}} = e^{+sT_{pd}} * \frac{v_{out}}{v_{in}} = e^{+sT_{pd}} * \frac{1}{\sum_{i=0}^{n} b_i s^i}$$

Let B_k be the coefficients of s^k in the new transfer function which gives the rise-time delay only.

$$\frac{v'_{out}}{v_{in}} = \frac{1}{\sum_{k=0}^{n} B_k s^k}$$

which yields

$$\sum_{k=0}^{n} B_k s^k = e^{-sT_{pd}} * \sum_{i=0}^{n} b_i s^i$$

Therefore, the new coefficients are given by

$$B_k = \sum_{i=0}^{k} b_i * \frac{(-T_{pd})^{k-i}}{(k-i)!}$$

So the first two coefficients of the new transfer function representing only the rise-time are:

$$B_0 = b_0, \qquad B_1 = b_1 - T_{pd}, \qquad B_2 = b_2 - T_{pd} b_1 + \frac{T_{pd}^2}{2}$$

Therefore, the rise-time of the response at any leaf of an interconnect tree can be calculated using these new coefficients in the two-pole response (Appendix A).